中国科学技术大学
University of Science and Technology of China

Recent results of baryon EMFFs at BESIII

周小蓉
中国科学技术大学

BESIII实验物理研讨会
Feb.5-8 2026, 北京

Introduction

Electromagnetic Form Factors (EMFFs)

- Electromagnetic Form Factors are fundamental properties of the nucleon
  - Connected to charge, current distribution
  - Crucial testing ground for models of the nucleon internal structure

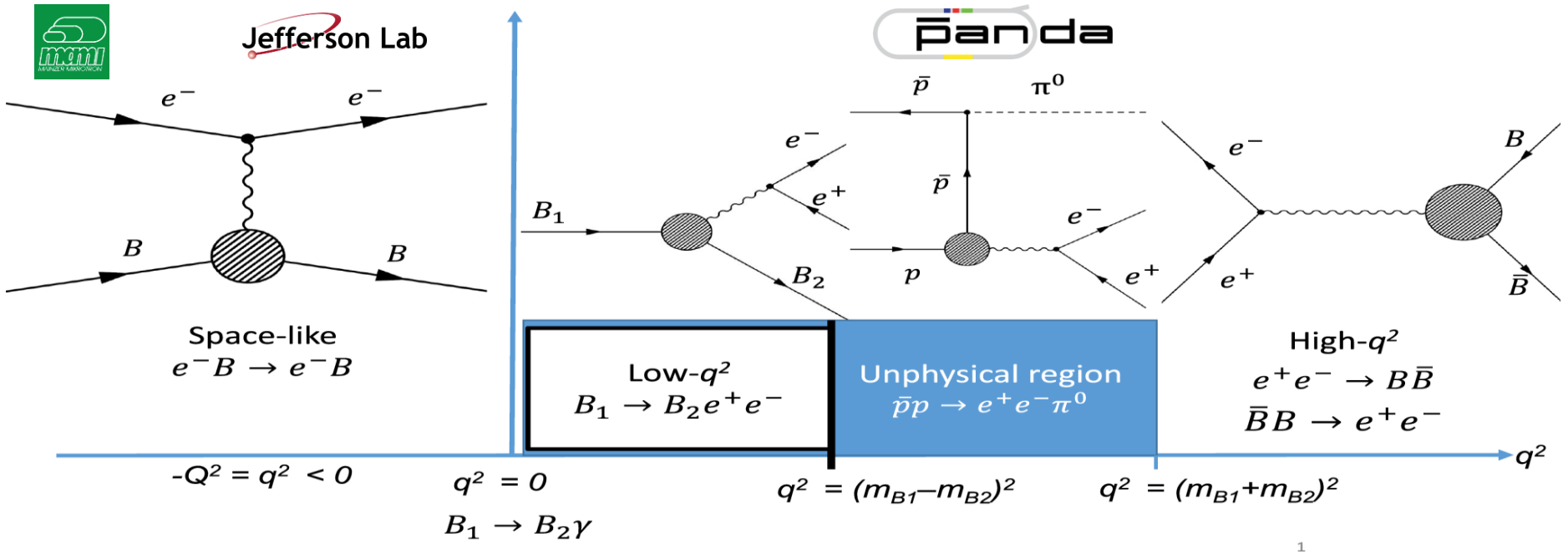

The nucleon electromagnetic vertex Γ_μ describing the hadron current:

$$\Gamma_\mu(p',p) = \gamma_\mu F_1(q^2) + \frac{i\sigma_{\mu\nu}q^\nu}{2m_p} F_2(q^2)$$

Sachs FFs: $G_E(q^2) = F_1(q^2) + \tau\kappa_p F_2(q^2)$, $G_M(q^2) = F_1(q^2) + \kappa_p F_2(q^2)$

Time-like EMFFs: formalism

- Interaction of final states, lead to a non-zero cross section for charged baryon at threshold.

Sov. Phys. Usp. **34** 375(1991)

$$\frac{d\sigma_{B\bar{B}}}{d\cos\theta} = \frac{\pi\alpha^2 C\beta}{2q^2}\left[(1+\cos^2\theta)|G_M|^2 + \frac{1}{\tau}|G_E|^2\sin^2\theta\right], \tau = \frac{q^2}{4m_B^2}$$

Integrated version: $\sigma_{B\bar{B}} = \frac{4\pi\alpha^2 C\beta}{3q^2}\left[|G_M|^2 + \frac{1}{2\tau}|G_E|^2\right]$

$$\xrightarrow{|G_E|=|G_M|} \sigma_{B\bar{B}} = \frac{2\pi\alpha^2 C\beta}{q^2}|G_{\text{eff}}|^2$$

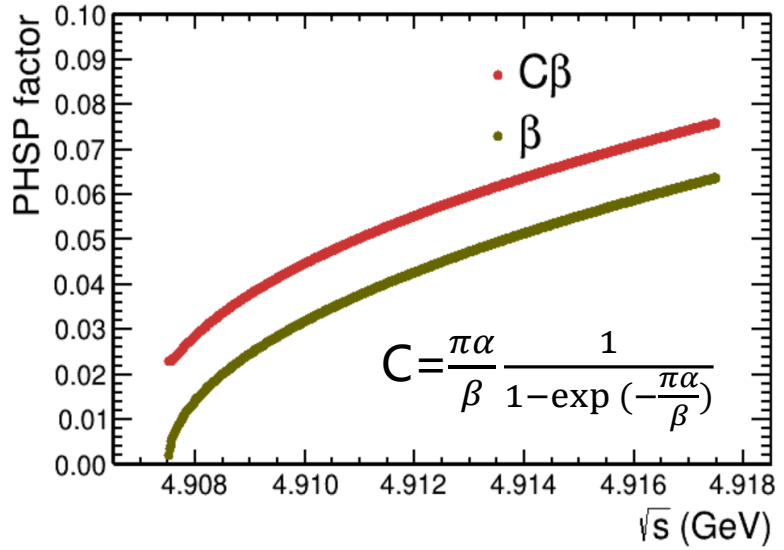

- Complex form of TLFFs leads to transversely polarized baryon even the beams are unpolarized

Nuov Cim A **109**, 241–256 (1996)

$$P_y = -\frac{\sin 2\theta\ \mathrm{Im}[G_E G_M^*]/\sqrt{\tau}}{\frac{|G_E|^2\sin^2\theta}{\tau} + |G_M|^2(1+\cos^2\theta)}$$

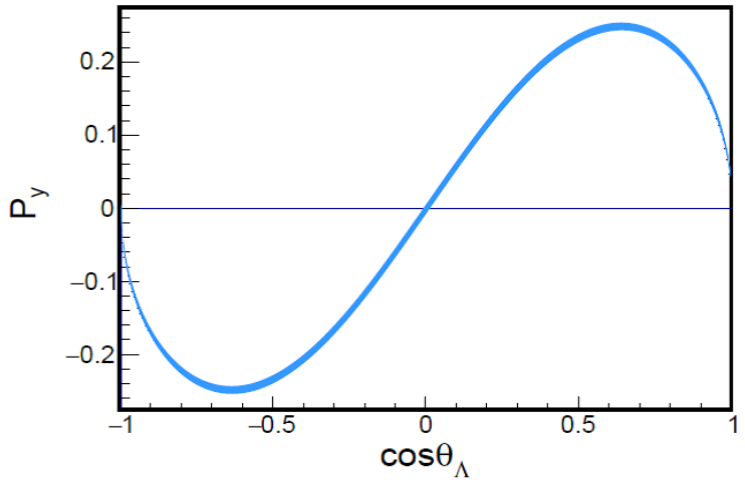

Time-like EMFFs: theoretic models

- Various theoretical models describe TLFF in non-perturbative region: ChEFT, VMD, Relativistic CQM, parton model, pQCD etc.

Parametrization of TLFF:

pQCD predicts continuous transition at high q^2, with the scaling behavior: $F_1 \propto q^{-4}, F_2 \propto q^{-6}$

Modified scaling expression in nonperturbative region: $\frac{q^2 F_2}{F_1} \propto \ln(\frac{q^2}{\Lambda^2})$, with $\Lambda \approx 0.3$ GeV

VMD model described the effect of meson cloud

$$|G_{\mathrm{eff}}| = \frac{\mathcal{A}}{q^4[\ln^2\left(\frac{q^2}{\Lambda^2}\right)+\pi^2]} \text{ or}$$

$$|G_{\mathrm{eff}}| = \frac{\mathcal{A}}{\left(1+\frac{q^2}{m_a^2}\right)[1-q^2/q_0^2]^2}$$

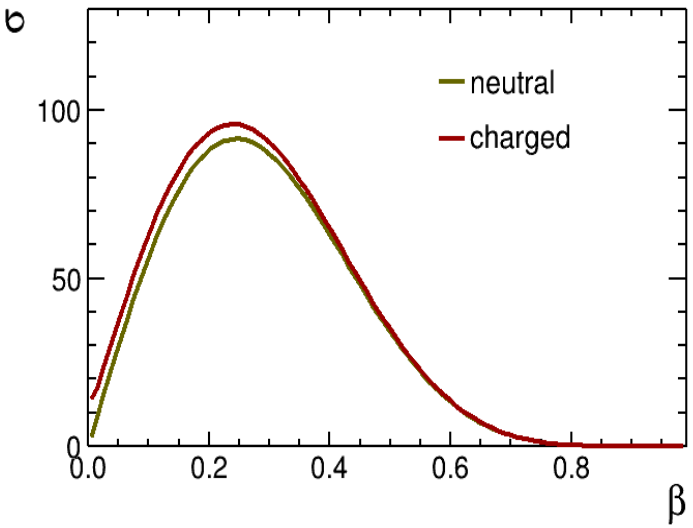

- Dispersion theoretical analysis, provide a coherent framework for the joint interpretation of SL and TL EMFFs over the entire physical range of q^2.

Time-like EMFFs: experimental approaches

- **Energy scan method at discrete c.m.energies**

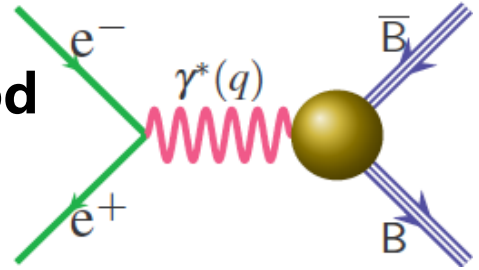

  - Well-defined c.m.energy, low background
  - Very good energy resolution
  - Discrete values, leaving gaps without information

- **Initial state radiation method at a fixed c.m.energy**

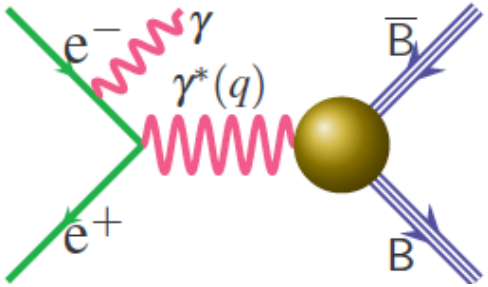

  - At a fixed c.m.energy $\sqrt{s}$, collecting events from threshold to $\sqrt{s}$
  - Systematic uncertainty in a coherent way
  - Large luminosity needed
  - Higher background

CLEO-c

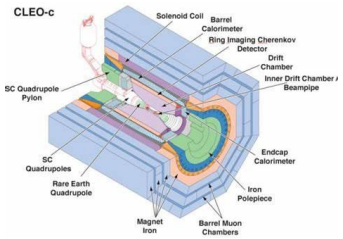

CMD-3

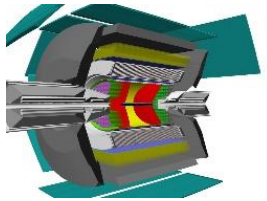

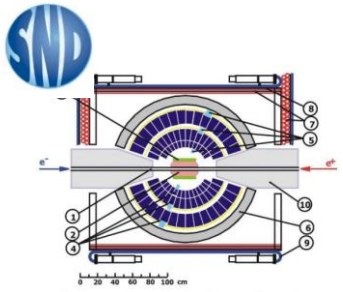

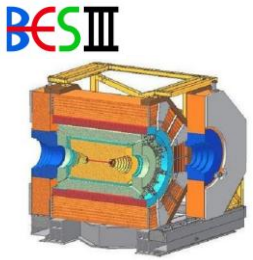

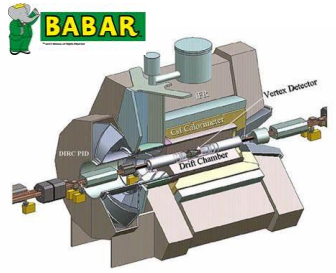

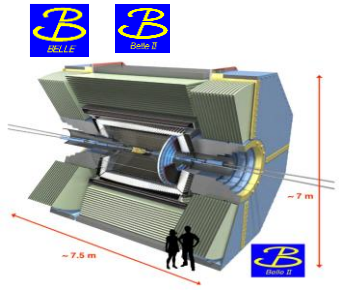

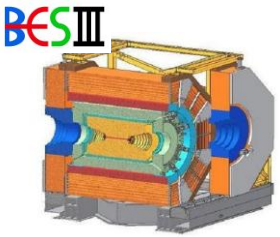

BESIII实验是唯一可以通过**能量扫描**和**初态辐射方法**同时研究类时重子形状因子的实验装置

Nucleons

Timeline of Proton EMFFs

Cross section

200 signal events in total, limited narrow energy region

BaBar observed threshold effect via ISR

BESIII & CMD obtained best precision via energy scan at >2.0 GeV and near threshold

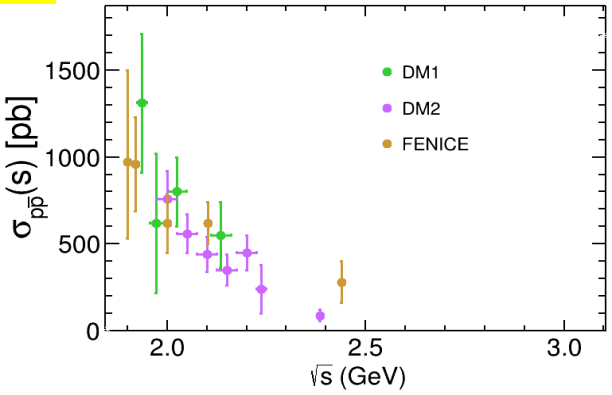

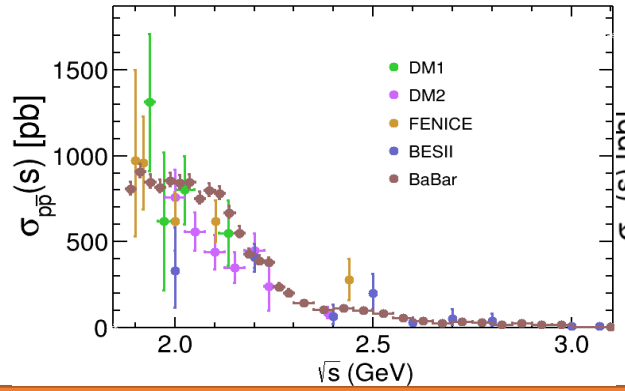

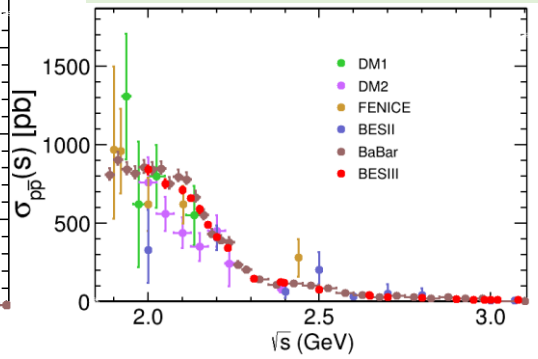

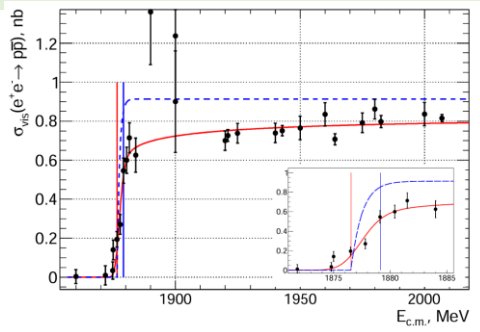

Year

$|G_E/G_M|$

Before 2000

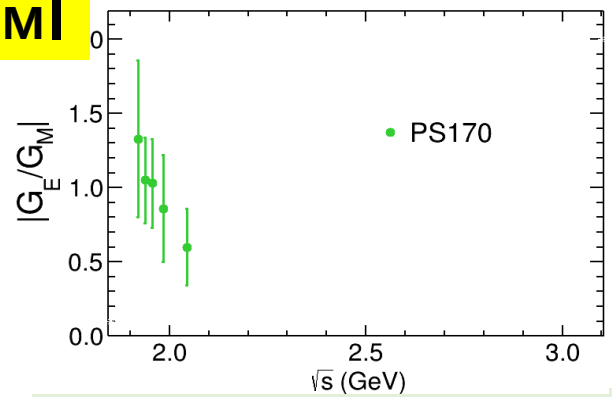

PS170 observed $|G_E/G_M|$ ratio for the first time at LEAR

2000 to 2020

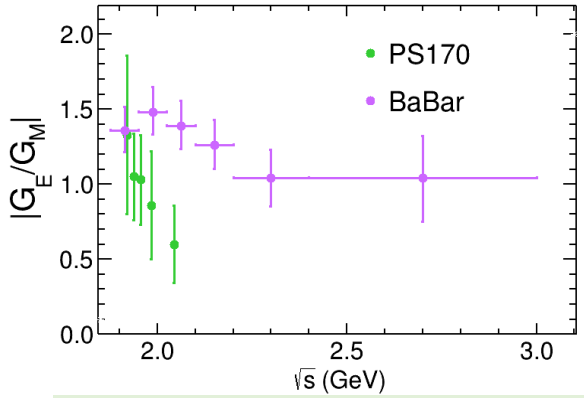

Result from BaBar is inconsistent with PS170

2020-2025

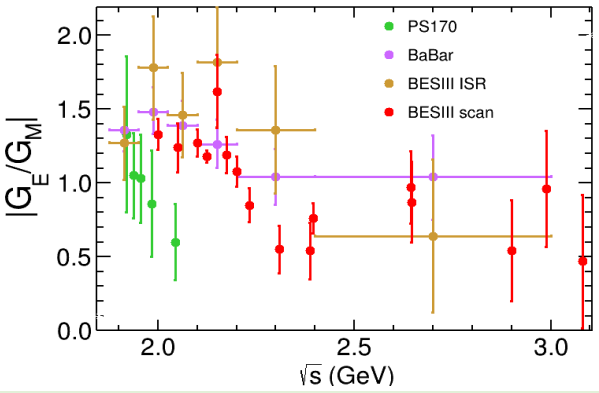

BESIII observed oscillation in the $|G_E/G_M|$ lineshape

New data near nucleon pair threshold 1.84-1.97 GeV

Recent results of proton EMFFs

- ISR method with detected photon and undetected at BESIII.
- **Damped oscillation** distribution after subtracting the modified dipole.

PLB 817, 136328 (2021)

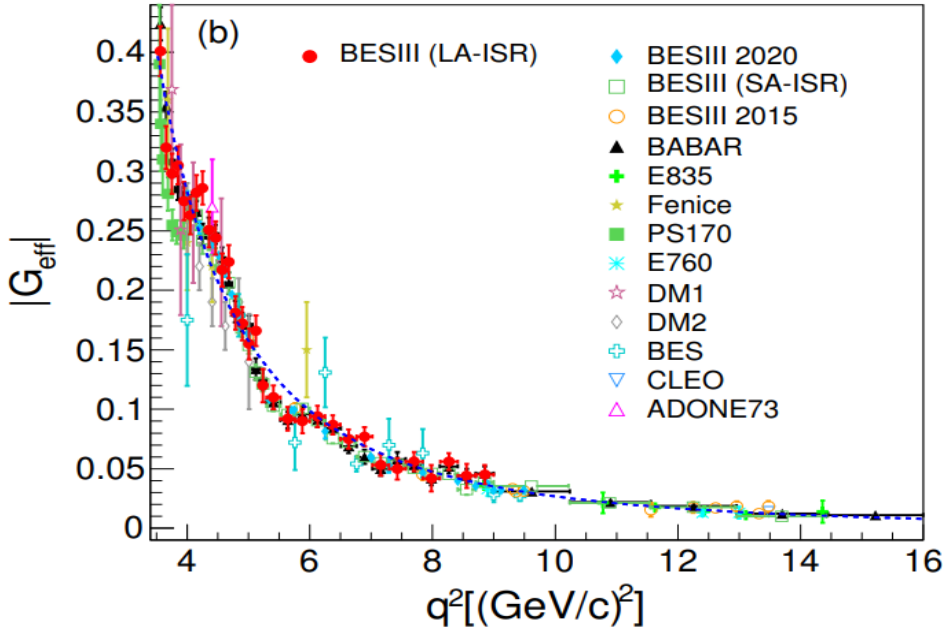

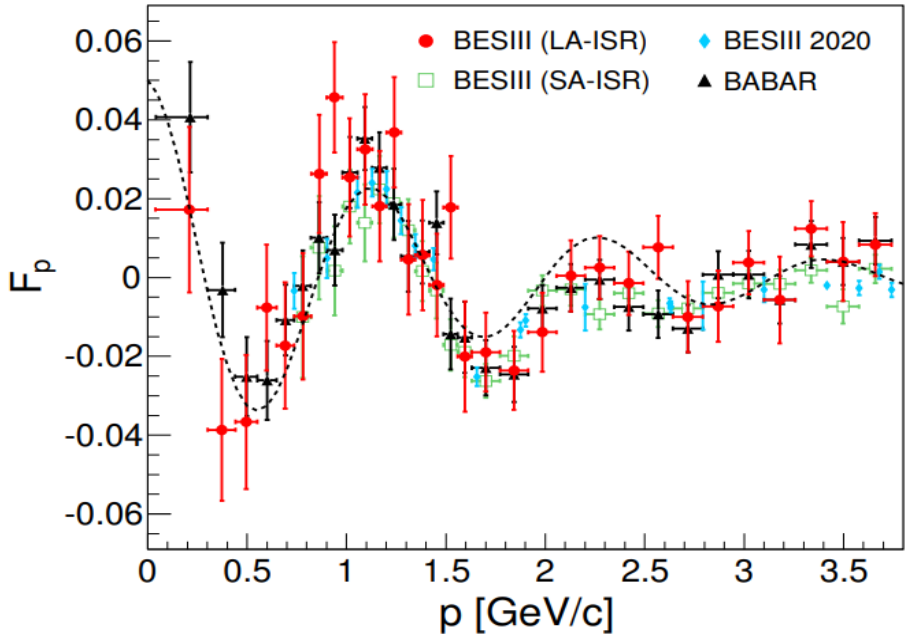

Blue dashec $|G_{\rm eff}| = \dfrac{\mathcal{A}}{(1+q^2/m_a^2)[1-q^2/q_0^2]^2},\ q_0^2 = 0.71\ ({\rm GeV}/c)^2,$

Black dashed: $F_p = A^{\rm osc}\exp(-B^{\rm osc}p)\cos(C^{\rm osc}p + D^{\rm osc}),$

Recent results of proton EMFFs

- Scan technique from $\sqrt{s} = 2.0$ to 3.08 GeV, using 688.5 pb^{-1} integrated luminosity.
- $|G_E/G_M|$, $|G_M|$ are determined with **high accuracy**, $|G_E|$ is measured for the first time.

PRL 124, 042001 (2020)

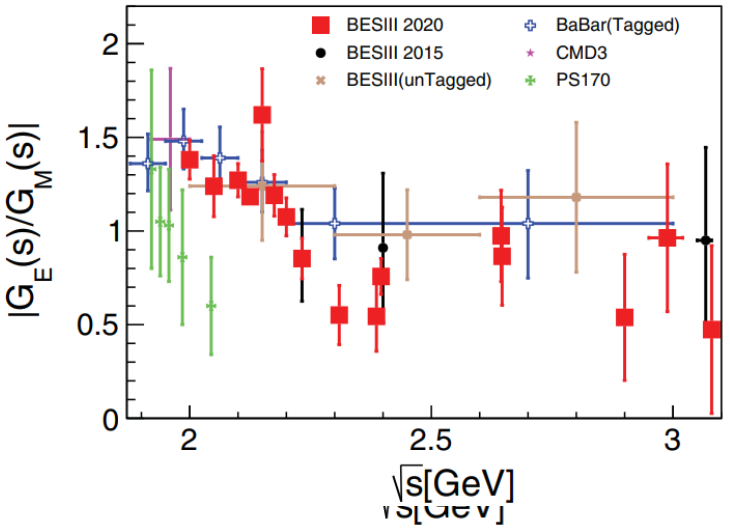

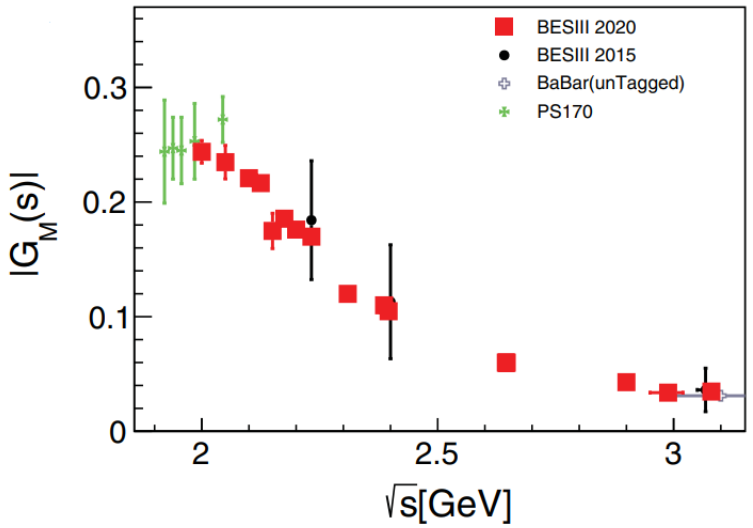

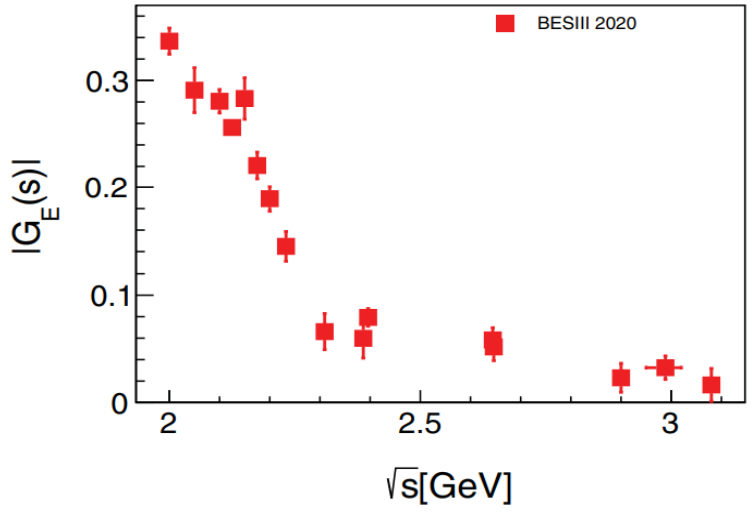

Analyticity of proton EMFFs

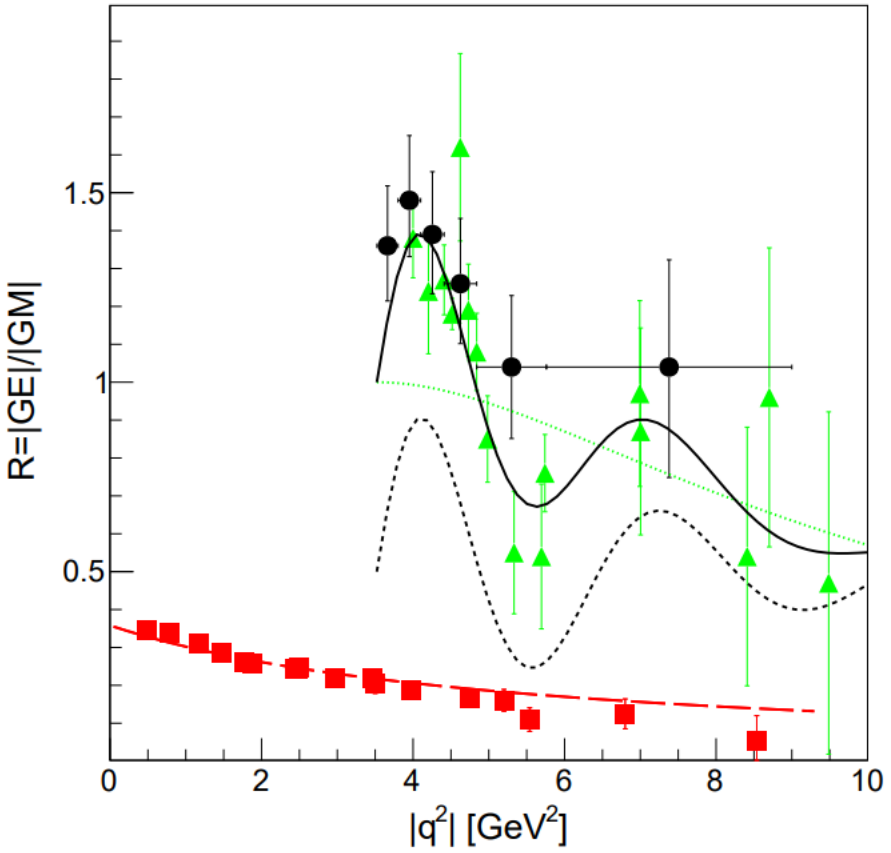

- SL data shows a monotone decrease from $1/\mu_p$ at $q^2 = 0$.
- TL data decreases from 1 at threshold $q^2 = 4m_p^2$.
- Damped oscillation feature of $|G_E/G_M|$ in Time-like

$$F_R(\omega(s)) = \frac{1}{1+\omega^2/r_0}\left[1 + r_1 e^{-r_2\omega}\sin(r_3\omega)\right],\ \omega = \sqrt{s} - 2m_p$$

- Perturbative domain has not been reached.

E. Tomasi-Gustafsson et al., PRC 103, 035203 (2021)

Timeline of Neutron EMFFs

Cross section

First result from FENICE, large cross

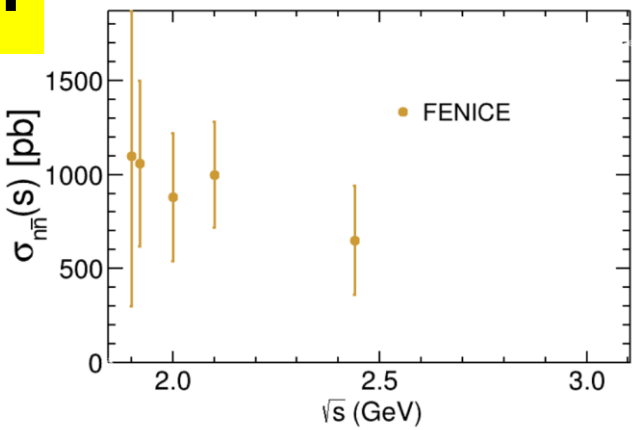

SND scan near threshold, plateau

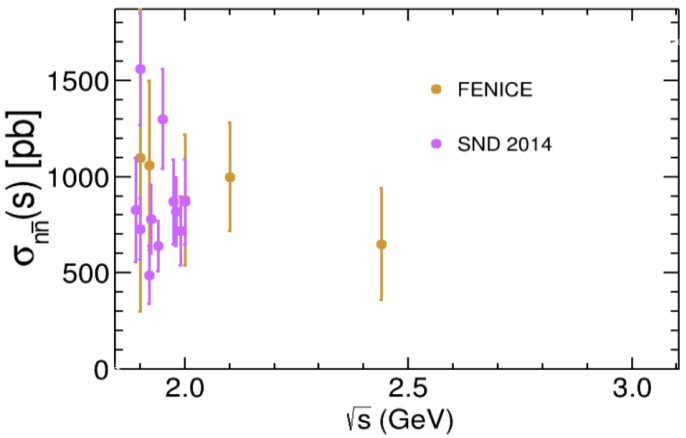

BESIII and SND obtain precise results

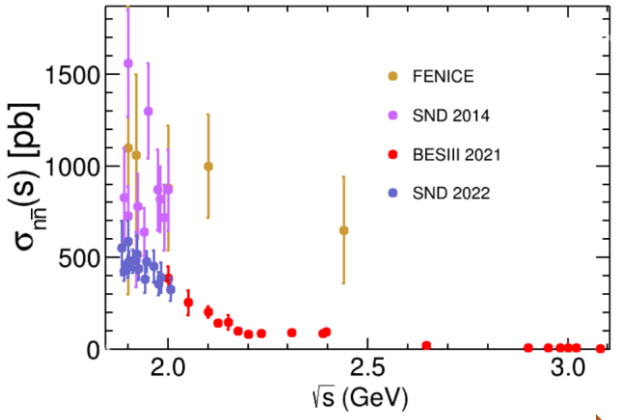

Before 2000 **2000 to 2020** **2020** **Year**

$|G_E/G_M|$

No experimental result

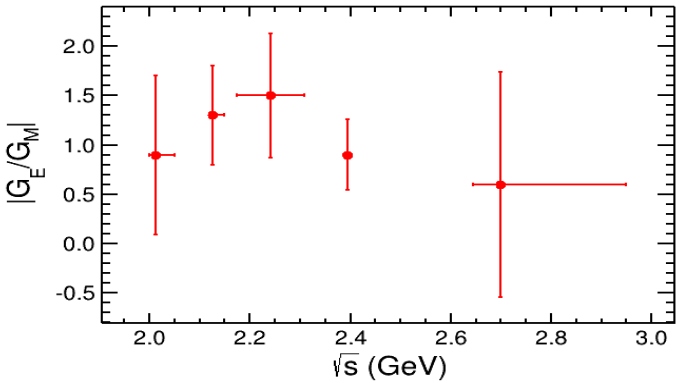

BESIII measured $|G_E/G_M|$ for the first time

Recent results of neutron EMFFs

- $e^+e^- \to n\bar{n}$ from $\sqrt{s}$ = 2.0-3.08 GeV, 647.9 pb^{-1}.
- $\gamma - p$ coupling larger than $\gamma - n$ coupling => consistent with theoretical limits from VMD, Skyrme etc.
- Oscillation of reduced-|G| observed in neutron with a phase orthogonal to that of proton.

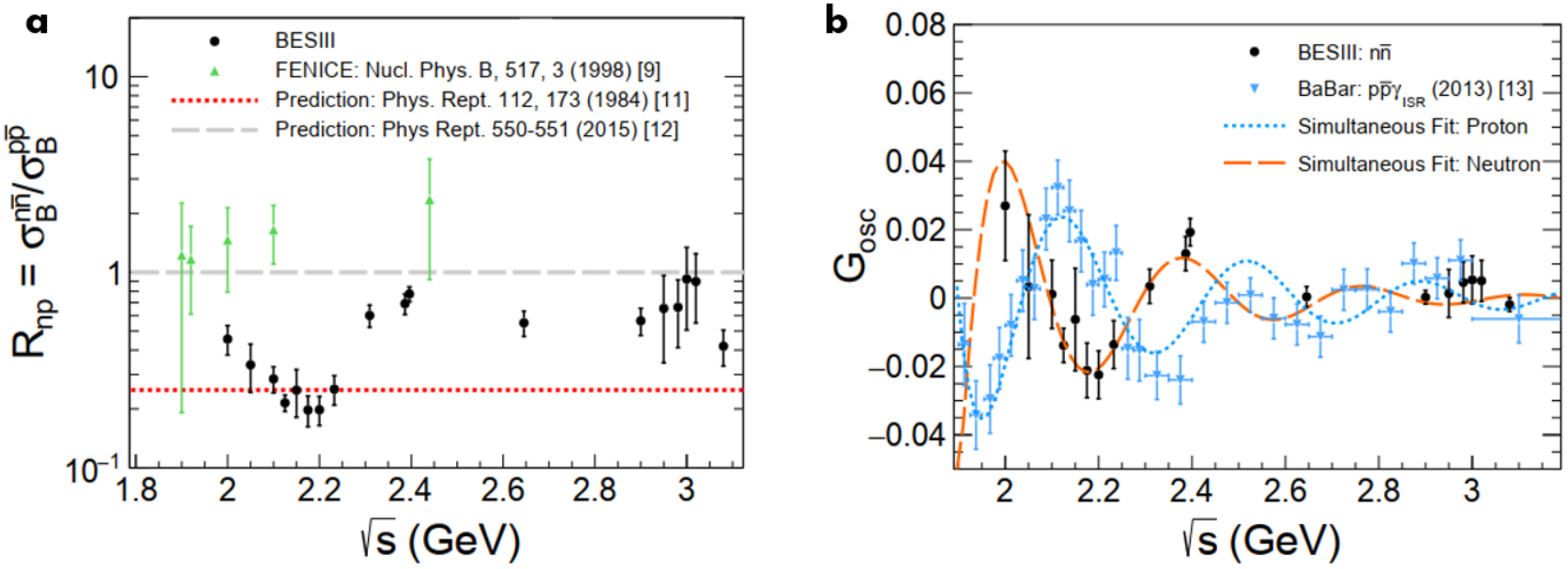

Nat. Phys. 17, 1200–1204 (2021)

Recent results of neutron EMFFs

- Compared with the FENICE results, the values for $|G_M|$ from this work are smaller by a factor of 2-3.
- Results is compared with various models: pQCD, modified dipole, VMD and dispersion relations (DR), and DR model gives good consistency.

PRL 130, 151905 (2023)

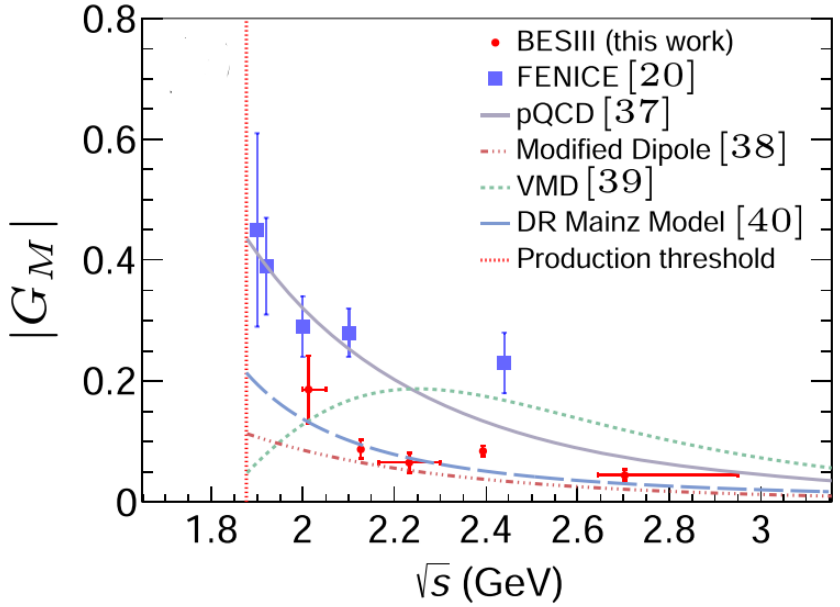

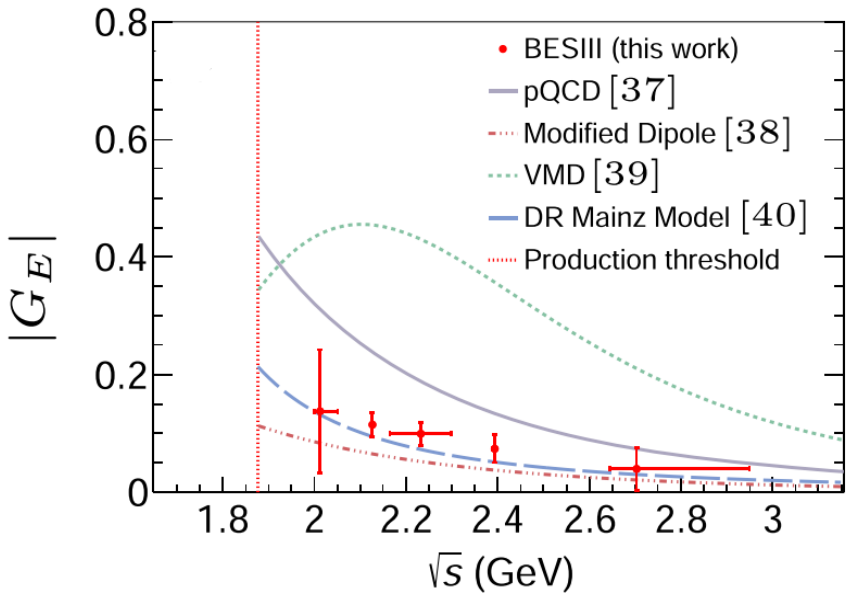

Hyperons

From nucleon to hyperon

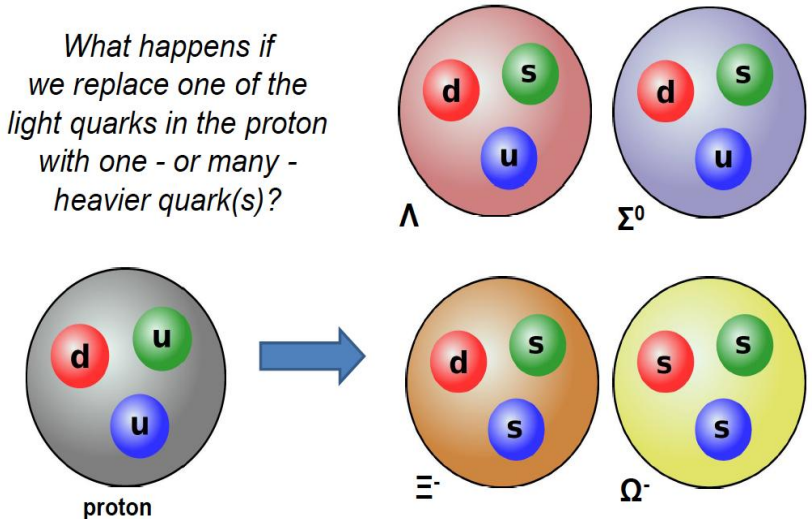

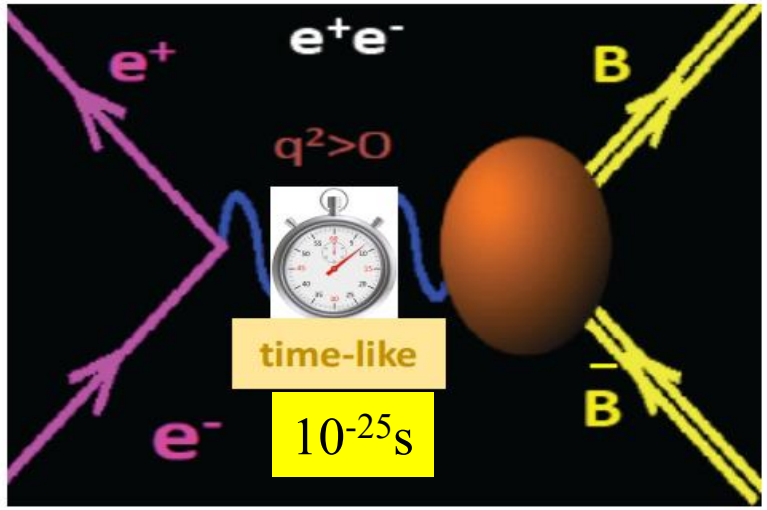

- The hyperons can be produced in e^+e^- annihilation above their production threshold
- Cross section can be obtained very close to threshold with finite PHSP of final state
- With hyperon weak decay to B+P, the polarization of hyperon can be measured, so does the relative phase between G_E and G_M

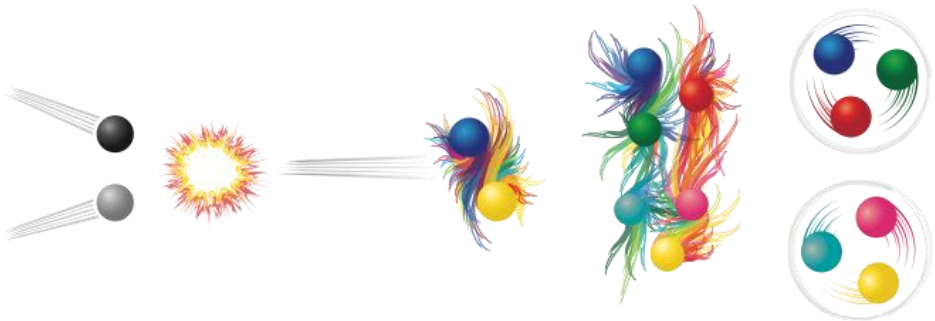

Cross section of $e^+e^- \to \Lambda\bar{\Lambda}$

- Let's recall the Born cross section for $e^+e^- \to B\bar{B}$:

$$\sigma_{B\bar{B}}(q) = \frac{4\pi\alpha^2 C\beta}{3q^2}\left[|G_M(q)|^2 + \frac{1}{2\tau}|G_E(q)|^2\right]$$

  - Coulomb factor: Charged $B\bar{B}$: $C=\frac{\pi\alpha}{\beta}\frac{1}{1-exp\,(-\frac{\pi\alpha}{\beta})}$, Neutral $B\bar{B}$: C=1
  - Near threshold, production cross section of neutral baryons should be zero

via Energy Scan

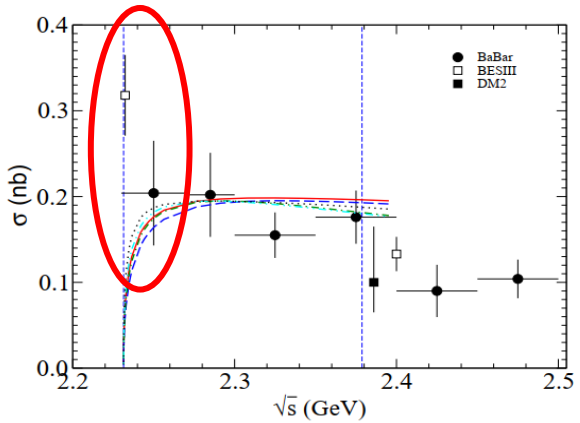

PRD 97, 032013 (2018)

via ISR

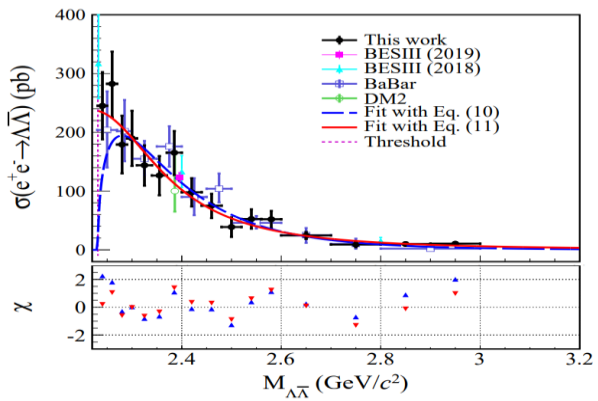

PRD 107, 072005 (2023)

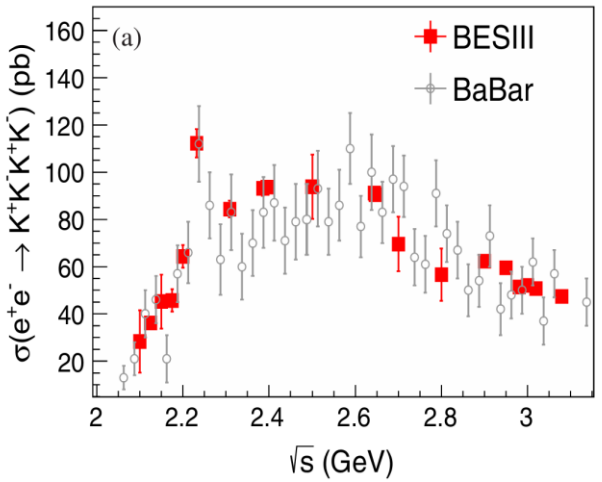

PRD100,032009(2019)

- The anomalous behavior differing from the pQCD prediction at threshold is observed

Relative phase of EMFFs

- In time-like region, EMFFs can be complex
- The non-zero relative phase between G_E and G_M gives transverse polarization of hyperons

$$P_y = -\frac{\sin 2\theta\ \mathrm{Im}[G_E G_M^*]/\sqrt{\tau}}{\frac{|G_E|^2 \sin^2\theta}{\tau} + |G_M|^2(1+\cos^2\theta)}$$

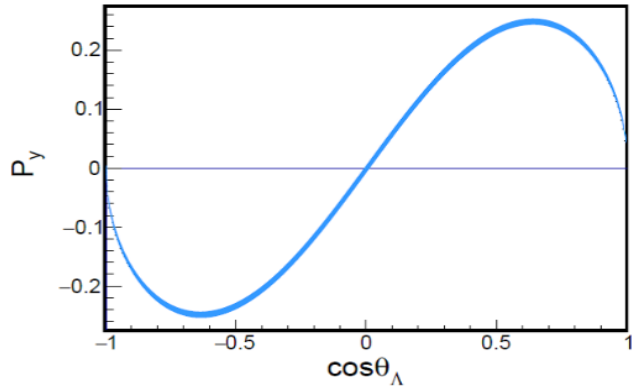

- The angular distribution of daughter baryon from Hyperon weak decay is:

$$\frac{d\sigma}{d\Omega} \propto 1 + \alpha_\Lambda P_y \cdot \hat{q}$$

α_Λ: asymmetry parameter

- Anisotropic proton decay distribution

$$\frac{dN}{d\cos\theta} = \frac{N_0}{2}(1 + \alpha_\Lambda P_\Lambda \cos\theta)$$

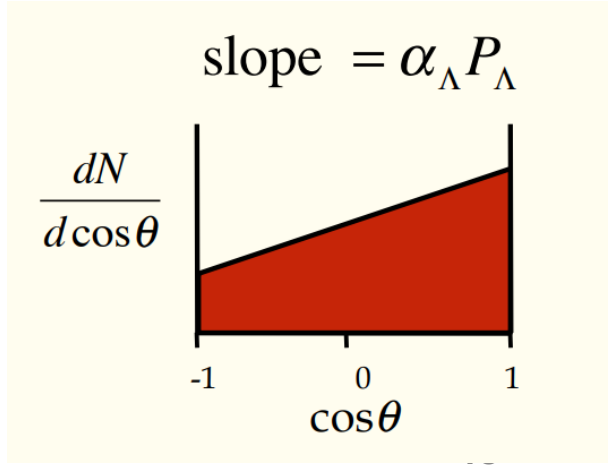

Relative phase of Λ EMFFs

- Matrix element of $e^+e^- \to J/\psi \to \Lambda\bar{\Lambda}$:

$$\mathcal{M} = F_1\gamma_\mu + \frac{F_2}{2m}q_\nu\sigma^{\nu\mu}\gamma_5 + i\epsilon^{\mu\nu\alpha\beta}\frac{\sigma_{\alpha\beta}}{4m}q_\nu F_3 + \frac{1}{2m}\left(q^\mu - \frac{q^2}{2m}\gamma^\mu\right)\gamma_5 F_4$$

- Differential cross section using spin density matrix and deca matrix
- A correlated 5-dim. angular distribution $\xi = (\theta_\Lambda, \theta_p, \phi_p, \theta_{\bar{p}}, \phi_{\bar{p}})$with 4 parameters is constructed

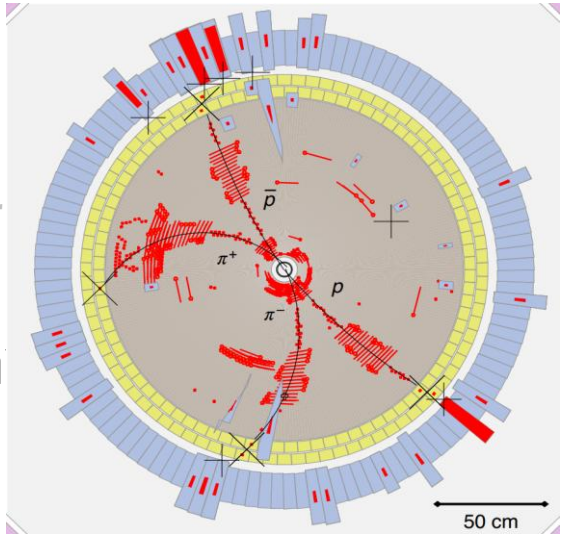

$$\omega(\xi, \Delta\Phi, \alpha_\psi, \alpha_-, \alpha_\gamma) = 1 + \alpha_\psi cos^2\theta_\Lambda$$ *Unpolarized part*

$$+\alpha_-\alpha_\gamma\left[sin^2\theta_\Lambda(n_{1,x}, n_{2,x} - \alpha_\psi n_{1,y}, n_{2,y}) + (cos^2\theta_\Lambda + \alpha_\psi)n_{1,z}, n_{2,z}\right]$$

$$+ \alpha_-\alpha_\gamma\sqrt{1-\alpha_\psi{}^2}\,cos(\Delta\Phi)\,sin\theta_\Lambda cos\theta_\Lambda(n_{1,x}, n_{2,z} + n_{1,z}, n_{2,x})$$ *Correlated part*

$$+\sqrt{1-\alpha_\psi{}^2}\,sin(\Delta\Phi)\,sin\theta_\Lambda cos\theta_\Lambda(\alpha_- n_{1,y} + \alpha_\gamma n_{2,y})$$ *Polarized part*

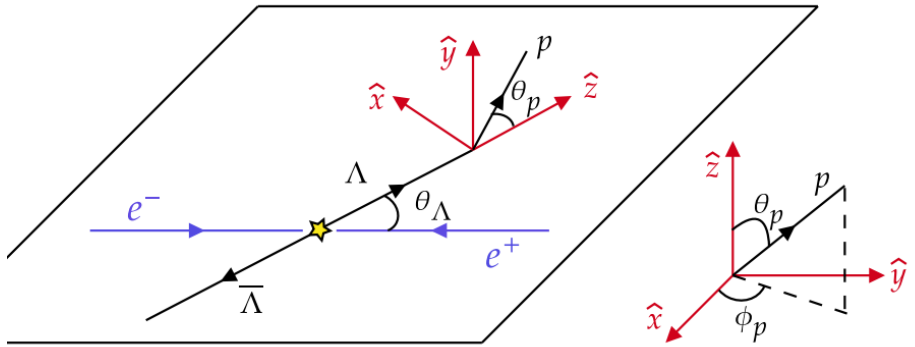

Relative phase of Λ EMFFs

@ 2.396 GeV

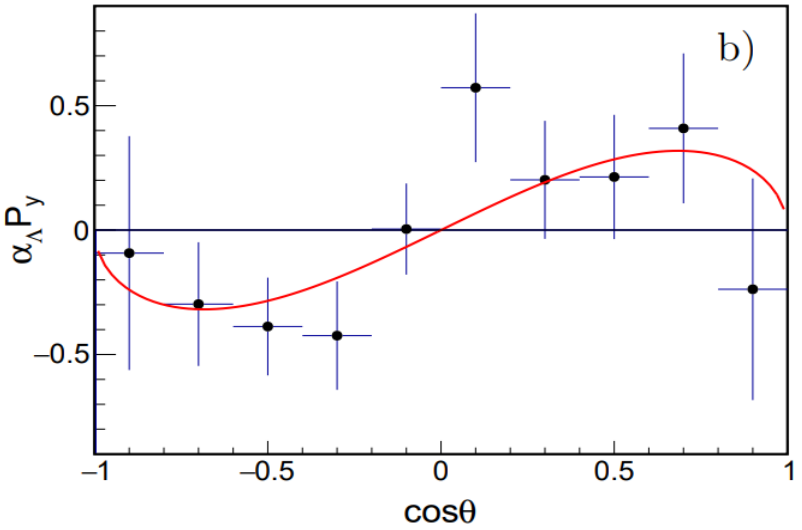

RPL 123, 122003 (2019)

$$\left|\frac{G_E}{G_M}\right| = 0.96 \pm 0.14(\text{stat.}) \pm 0.02(\text{sys.})$$

$$\Delta\Phi = 37^\circ \pm 12^\circ(\text{stat.}) \pm 6^\circ(\text{sys.})$$

(Confirm the complex form of EMFFs)

@ 2.3864-3.08 GeV

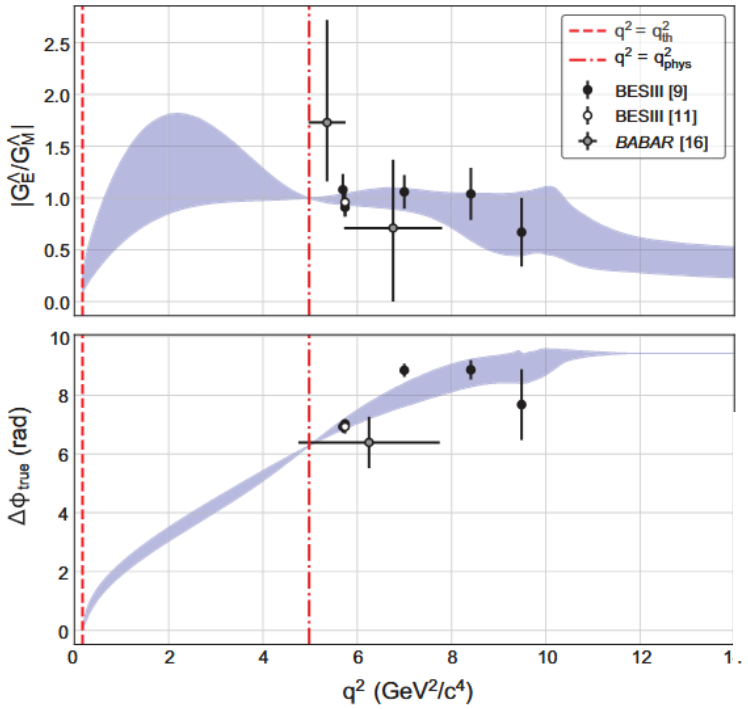

Energy	G_{eff}	R	$\Delta\Phi$ (°)
2.3864	0.1307(22)(14)	1.08(15)(03)	37(12)(01)
2.3960	0.1233(13)(13)	0.91(08)(02)	42(10)(02)
2.6454	0.0586(10)(07)	1.06(16)(03)	147(13)(01)
2.9000	0.0319(09)(06)	1.04(25)(03)	148(19)(01)
2.9500	0.0295(22)(04)	...	...
2.9810	0.0305(22)(04)	...	...
3.0000	0.0294(25)(04)	...	...
3.0200	0.0262(23)(05)	...	...
3.0800	0.0240(10)(05)	0.67(33)(03)	80(69)(02)

	6th, $\chi^2/\nu = 2.5$		7th, $\chi^2/\nu = 1.9$		8th, $\chi^2/\nu = 1.9$	
$(N_{\text{th}}, N_{\text{asy}})$	$\bar{r}_E^\Lambda$	P	$\bar{r}_E^\Lambda$	P	$\bar{r}_E^\Lambda$	P
(0,3)	-0.125 (70)	57	-0.076 (43)	83	-0.077 (40)	85
(0,4)	-0.109 (62)	26	-0.040 (30)	12	-0.040 (30)	7.6
(1,3)	0.070 (30)	8.0	0.031 (06)	3.0	0.055 (28)	3.8
(-1,1)	0.152 (59)	5.0	0.025 (19)	1.0	0.019 (16)	1.0

PRL 135, 191902 (2025)

Prediction of Λ EMFFs

PRD 103, 014028 (2021)

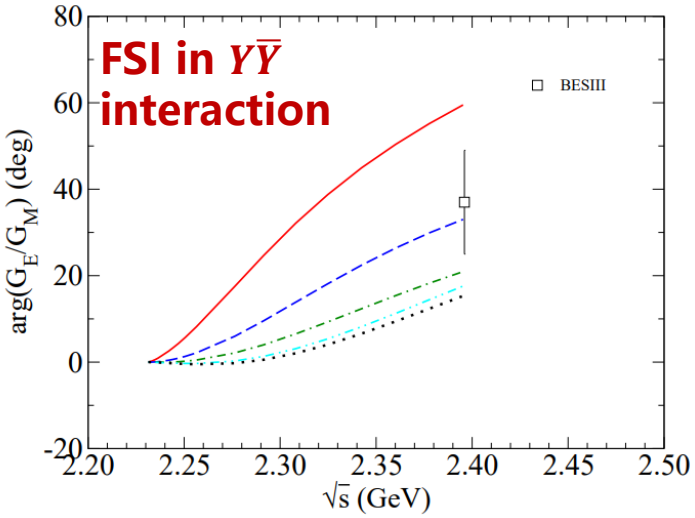

PRD 100, 073007(2019)

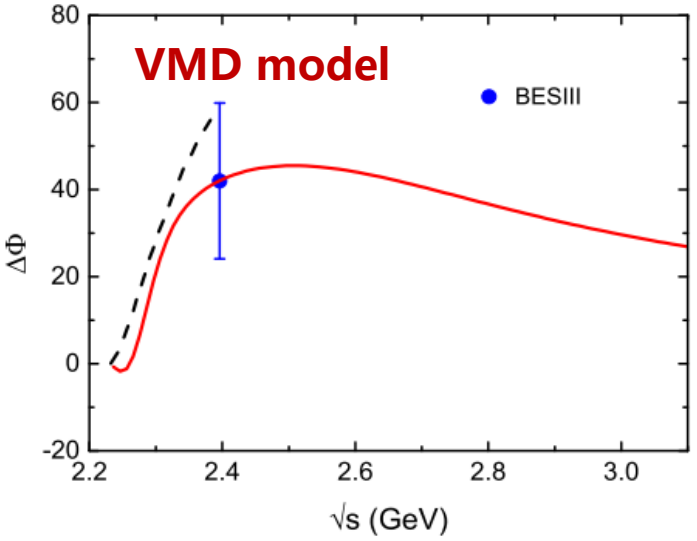

Dispersion relations *PRD 104,116016 (2021)*

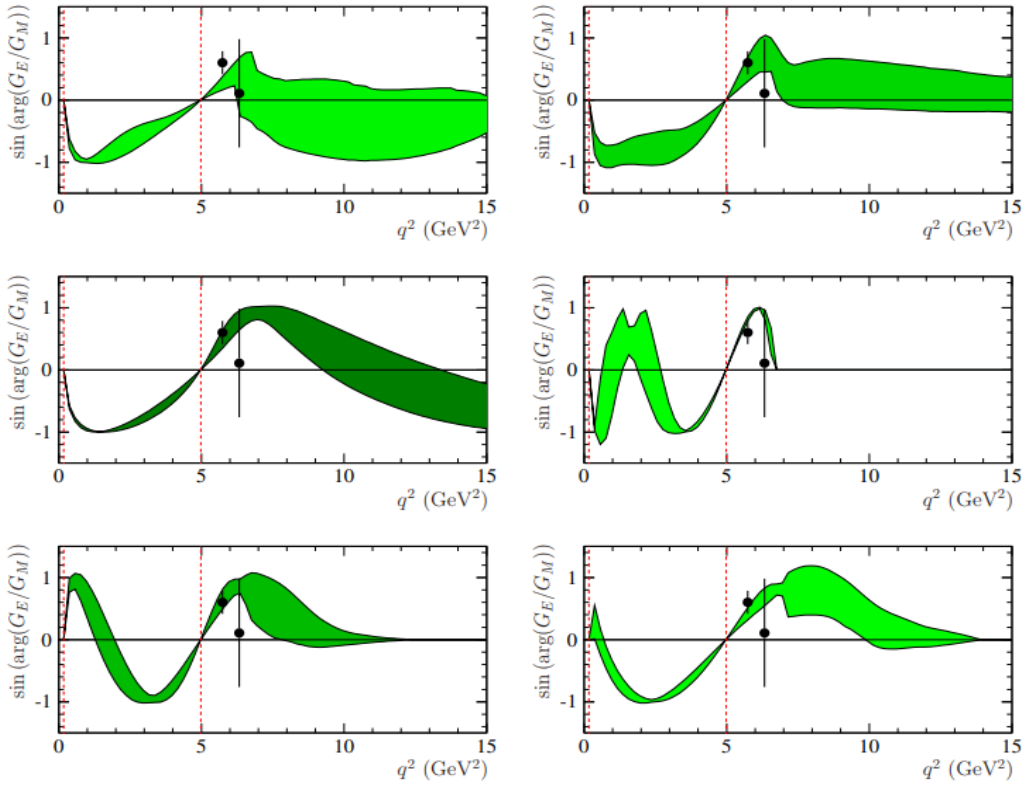

- Measurement of relative phase in a wide q^2 range would be crucial to enhance the predictive power of various model and test its asymptotic behavior in TL.

Cross section of $e^+e^- \to \bar{\Lambda}\Sigma^0 + c.c$

PRD 109,012002(2024)

- Nonzero Born cross section is observed at threshold, 72.9±12.6±5.4 pb
- Fit function 1: $\sigma^{\mathrm{B}}(s) = \dfrac{c_0 \cdot \beta \cdot \mathcal{C}}{(\sqrt{s} - c_1)^{10}}$,
- Fit function 2: $\sigma^{\mathrm{B}}(s) = \dfrac{e^{a_0}\pi^2\alpha^3\hbar^2c^2}{s\left[1 - e^{-\frac{\pi\alpha_s(s)}{\beta(s)}}\right]\left[1 + \left(\frac{\sqrt{s}-(m_\Lambda + m_{\bar{\Sigma}^0})c^2}{a_1}\right)^{a_2}\right]}$.

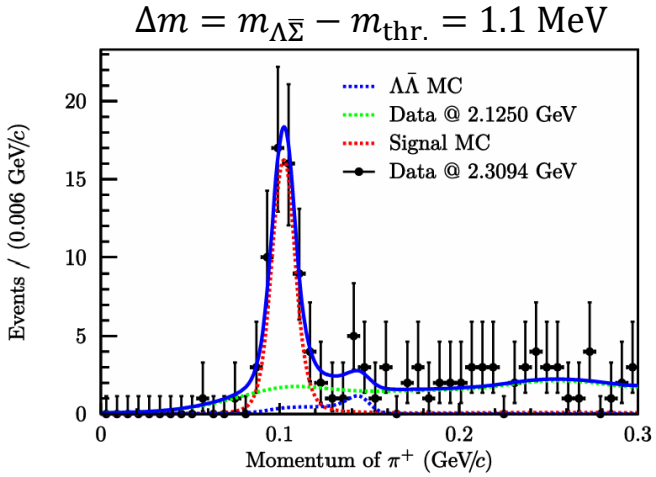

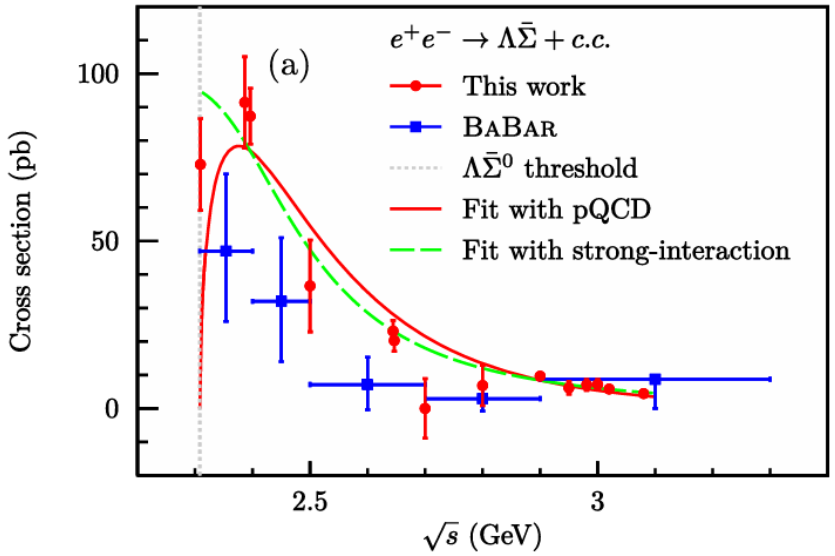

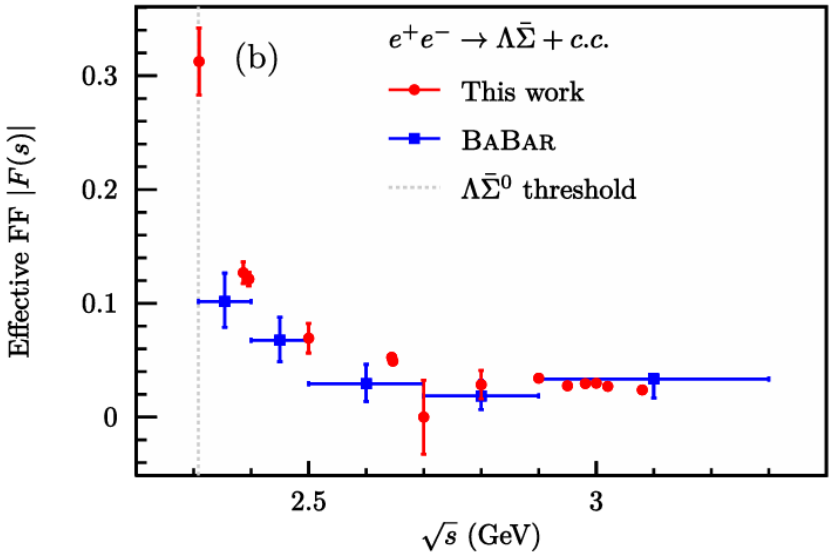

Cross section of $e^+e^- \to \Sigma\bar{\Sigma}$

- Born cross sections of $e^+e^- \to \Sigma^+\bar{\Sigma}^-, \Sigma^-\bar{\Sigma}^+, \Sigma^0\bar{\Sigma}^0$ are measured from threshold to 3.02 GeV
- The decay process of $\Sigma^+ \to p\pi^0, \Sigma^- \to n\pi^-, \Sigma^0 \to \gamma\Lambda$ are reconstructed
- None zero cross section near threshold observed for $\Sigma^+\bar{\Sigma}^-, \Sigma^-\bar{\Sigma}^+$ processes

$\Sigma^+\bar{\Sigma}^-$: $\Delta m = 7.76$ MeV

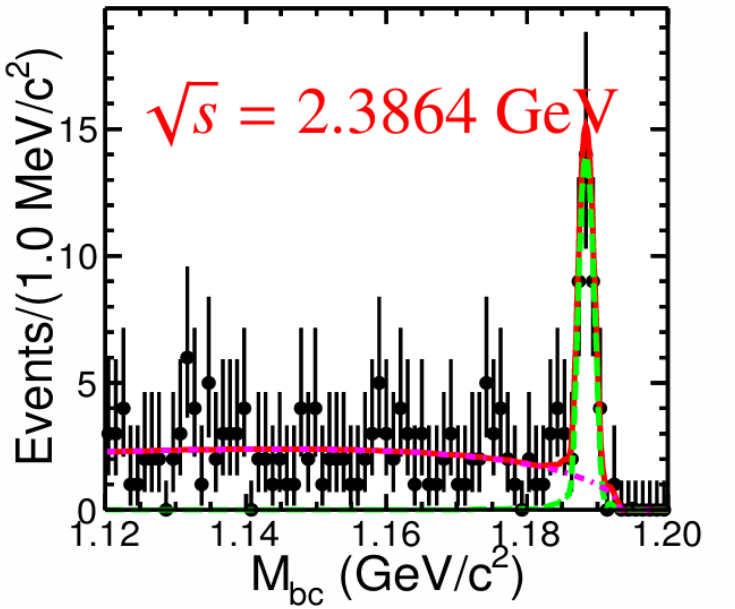

$\Sigma^-\bar{\Sigma}^+$: $\Delta m = 1.1$ MeV

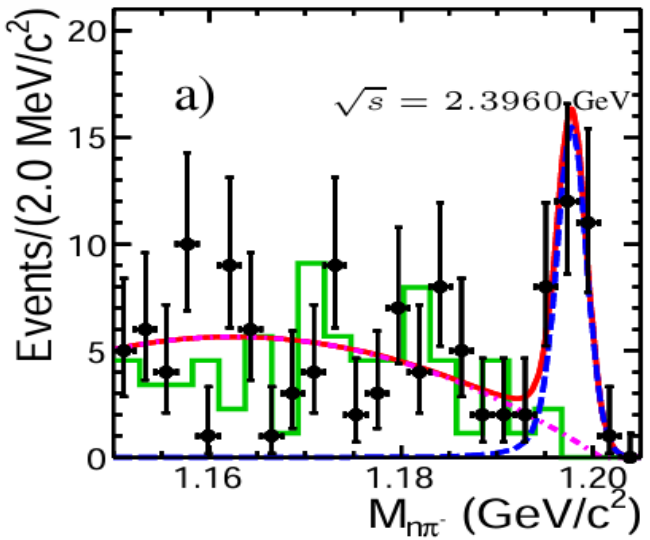

$\Sigma^0\bar{\Sigma}^0$: $\Delta m = 1.1$ MeV

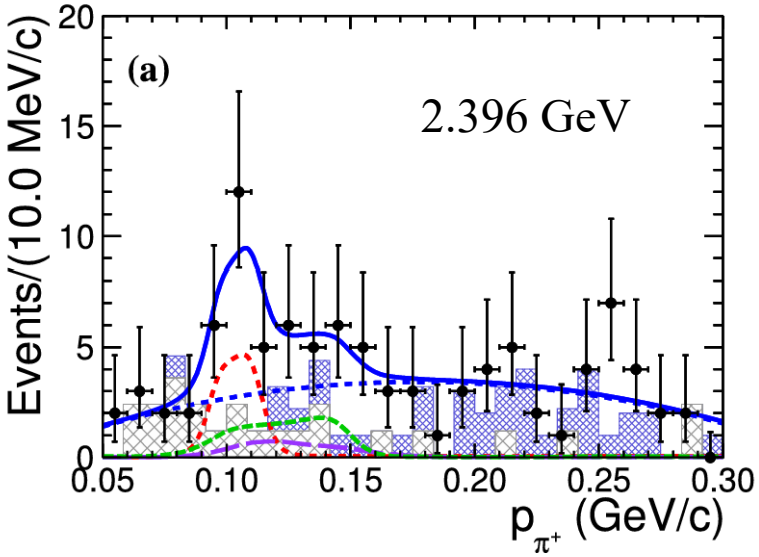

$\Sigma^\pm\bar{\Sigma}^\mp$:PLB 814, 136110 (2021)
$\Sigma^0\bar{\Sigma}^0$:PLB 831, 137187 (2022)

Cross section of $e^+e^- \to \Sigma\bar{\Sigma}$

- Born cross sections of $e^+e^- \to \Sigma^+\bar{\Sigma}^-, \Sigma^-\bar{\Sigma}^+, \Sigma^0\bar{\Sigma}^0$ are measured from threshold to 3.02 GeV
  - The cross sections can be well described by pQCD-motivated functions

$$\sigma^{\mathrm{B}}(s) = \frac{\beta C}{s}\left(1+\frac{2m_B^2}{s}\right)\frac{c_0}{(s-c_1)^4(\pi^2+\ln^2(s/\Lambda_{\mathrm{QCD}}^2))^2}$$

  - An asymmetry in cross sections for Σ isospin triplets: $9.7 \pm 1.3 : 3.3 \pm 0.7 : 1$ =>related with valence quark?

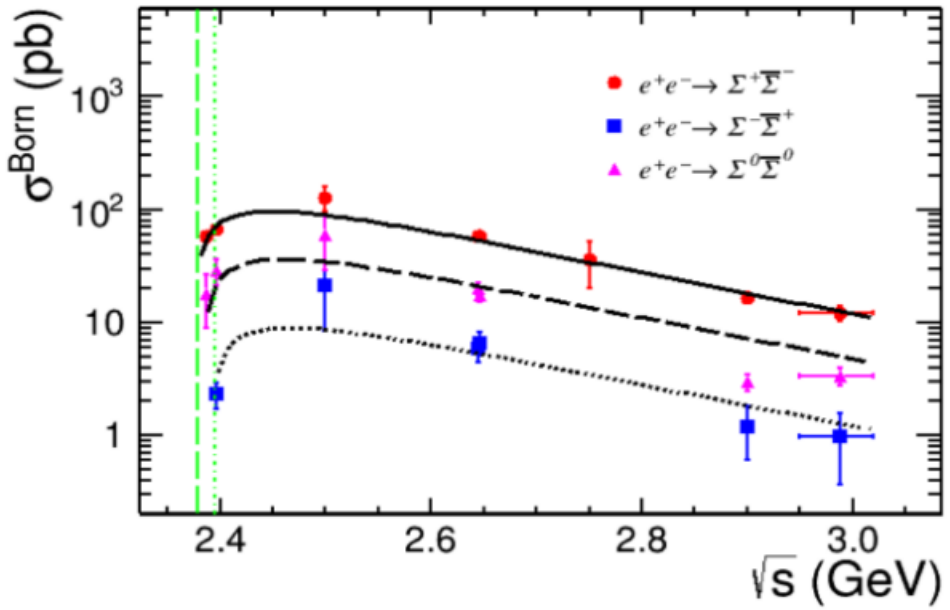

$\Sigma^{\pm}\bar{\Sigma}^{\mp}$:PLB 814, 136110 (2021)
$\Sigma^0\bar{\Sigma}^0$:PLB 831, 137187 (2022)

Relative phase of Σ^+ EMFFs

- An event of the reaction $e^+e^- \to \Sigma^+(\to p\pi^0)\bar{\Sigma}^-(\to \bar{p}\pi^0)$ is formalized by the similar joint angular distribution.
- Polarization is observed at $\sqrt{s}$ =2.396, 2.644 and 2.90 GeV with a significance of 2.2σ, 3.6σ and 4.1σ.
- Relative phase is determined for the first time in a wide q^2 range.

PRL132,081904 (2024)

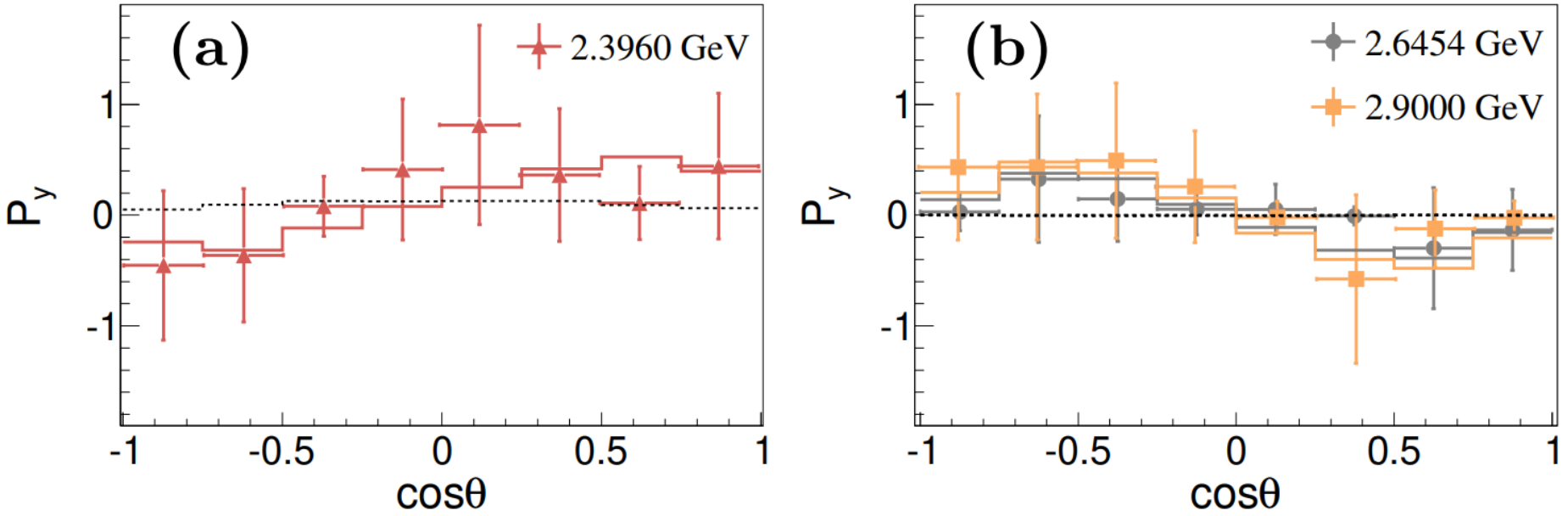

Complete measurement of Σ^+ EMFF

- $|G_E/G_M|$ and $\Delta\Phi$ line-shape is compared with $\bar{Y}Y$ model different tendency in $\Delta\Phi$.
- $\Delta\Phi$ distribution indicates there are integer multiples of π radians, from threshold to cross point.
- The still increasing relative phase indicates the asymptotic threshold has not yet been reached.

PRL132,081904 (2024)

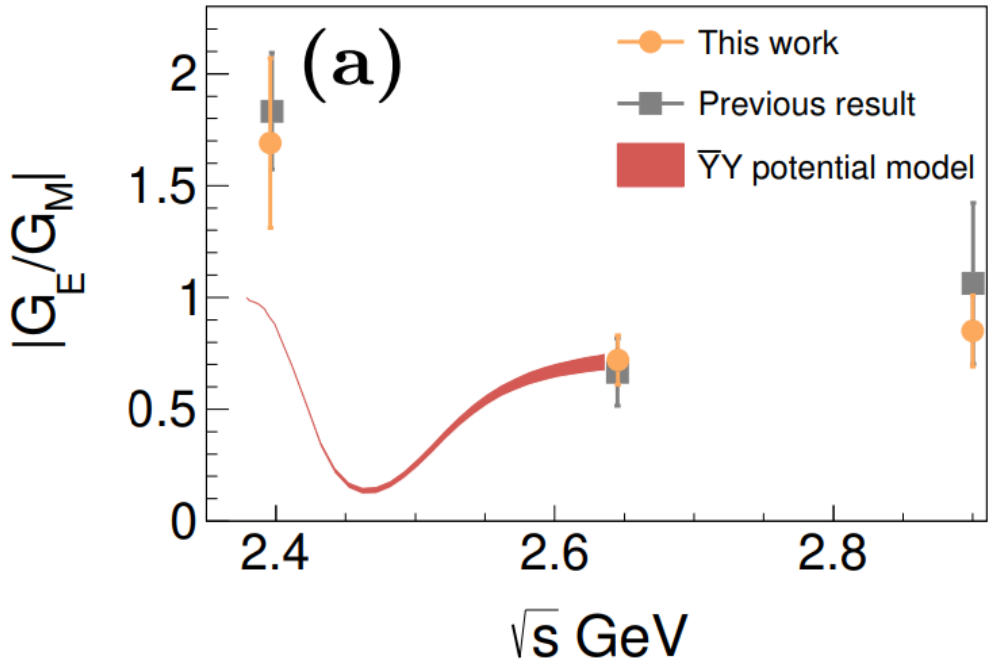

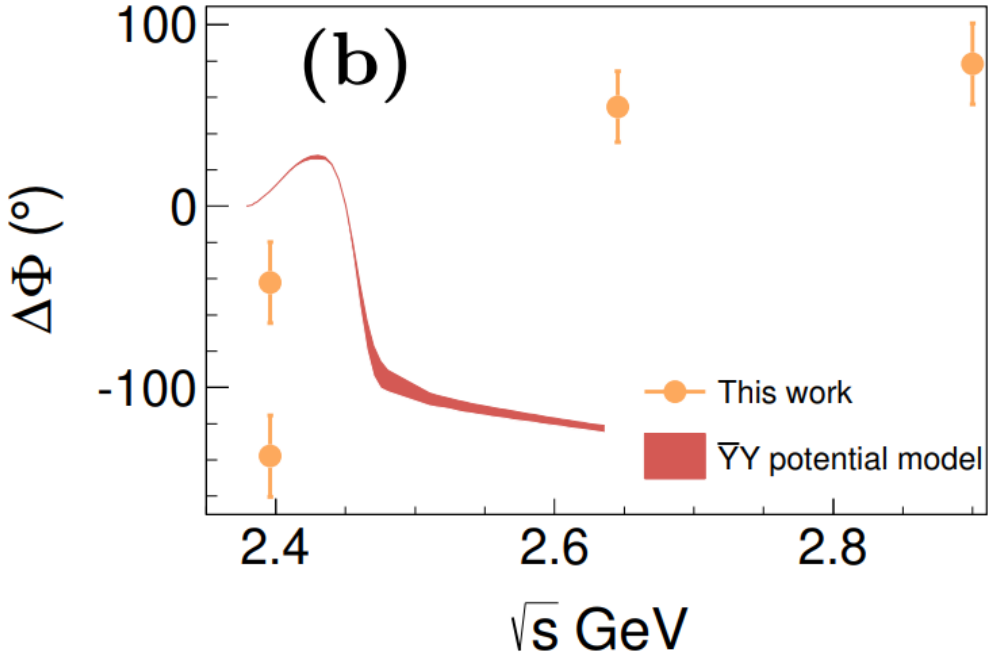

Cross section of $e^+e^- \to \Xi\bar{\Xi}$

$\Xi^0\bar{\Xi}^0$:PLB 820, 136557 (2021)
$\Xi^-\bar{\Xi}^+$:PRD103, 012005(2021)

- Born cross sections of $e^+e^- \to \Xi^0\bar{\Xi}^0$ and $\Xi^-\bar{\Xi}^+$ are measured from threshold to 3.08 GeV
  - No significant threshold enhancement observed
  - The ratio of Born cross sections for both modes agrees with the expectation of isospin symmetry.

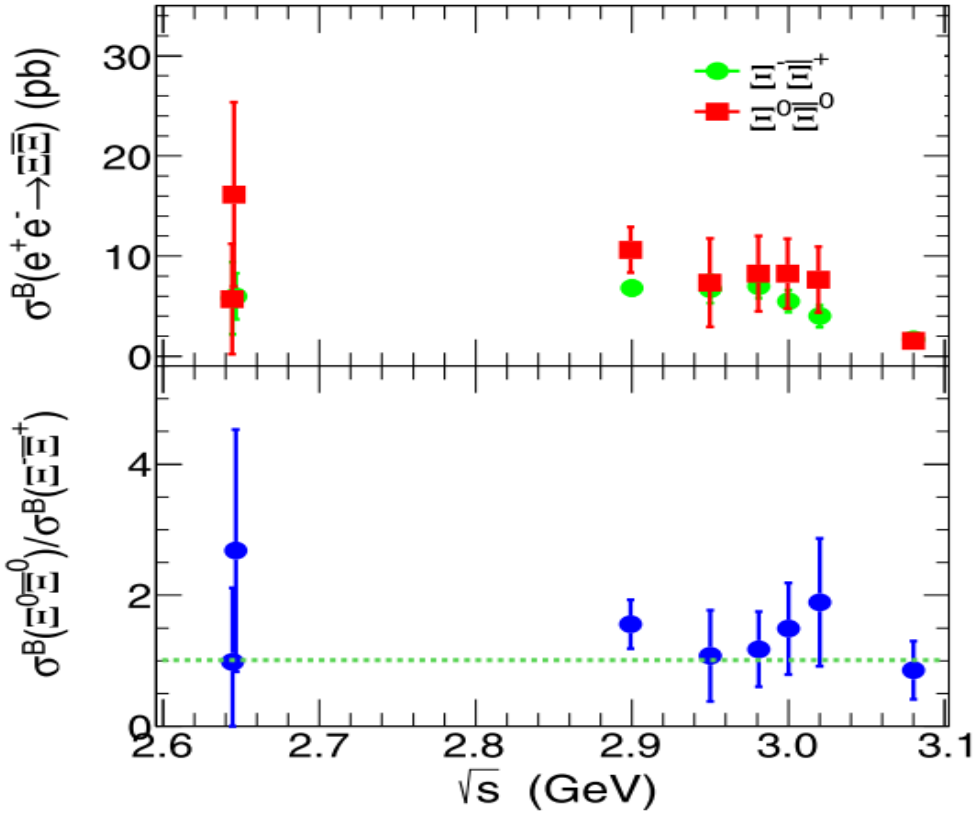

Cross section of $e^+e^- \to \Omega\bar{\Omega}/\Delta\bar{\Delta}$

- Born cross sections of $e^+e^- \to \Omega^-\bar{\Omega}^+$ at 8 energy points between $\sqrt{s} = 3.49$ and 3.67 GeV.
- No significant signal observed.
- Upper limit of effective FF is consistent with pQCD driven prediction.

PRD 107, 052003, 2023

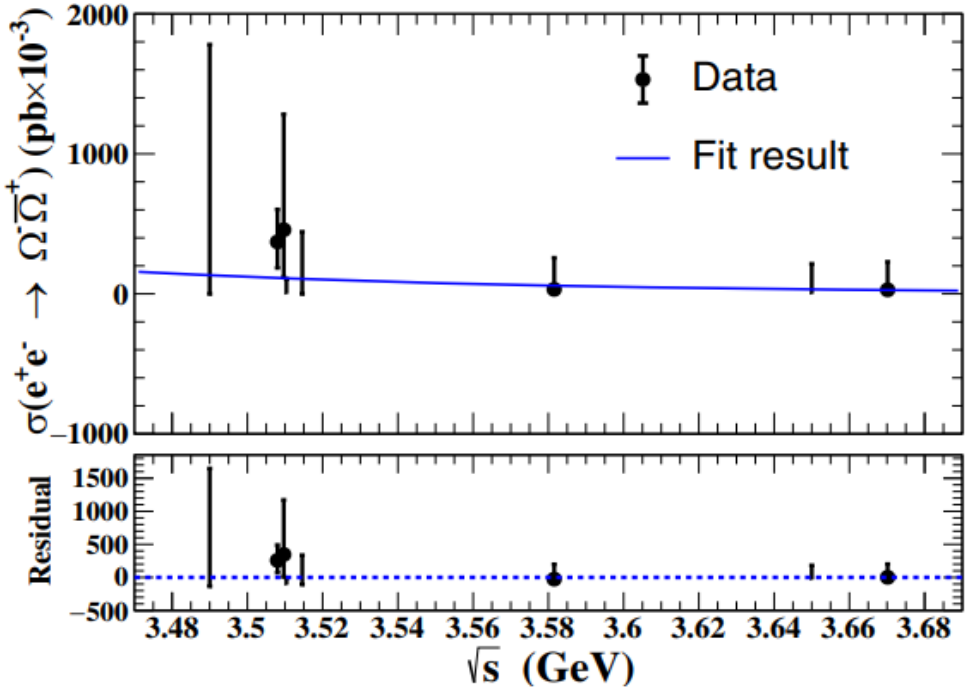

- $e^+e^- \to \Delta^{++}\bar{\Delta}^{--}$ is searched with c.m.s in 2.3094 to 2.6464 GeV.
- No significant signal observed, but signal for $e^+e^- \to \Delta^{++}\mathrm{p}\pi^-$ observed.

PRD 108, 072010(2023)

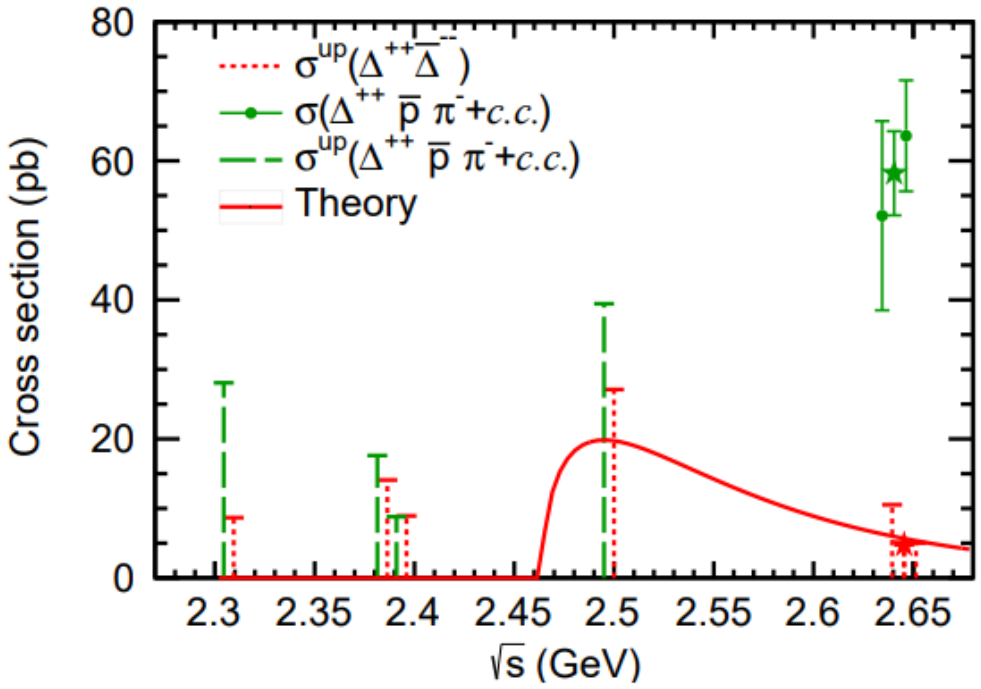

Charmed baryons

Cross section of $e^+e^- \to \Lambda_c^+\bar{\Lambda}_c^-$

- The BESIII measurements indicate that there is indeed a step in $e^+e^- \to \Lambda_c^+\bar{\Lambda}_c^-$, similar to $e^+e^- \to p\bar{p}$, followed by a plateau.

PRL 120, 132001 (2018)

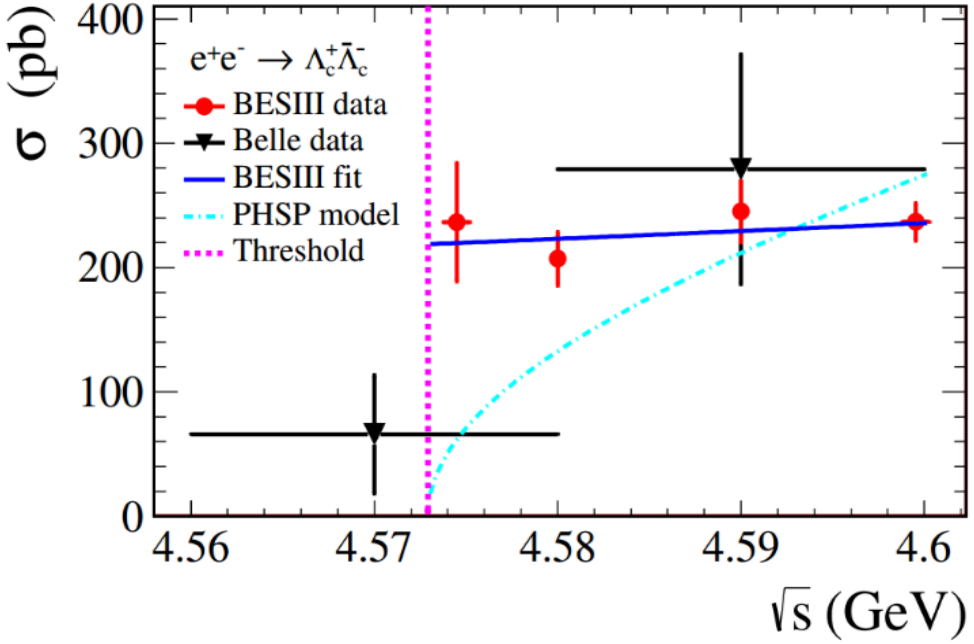

PRL131,191901 (2023)

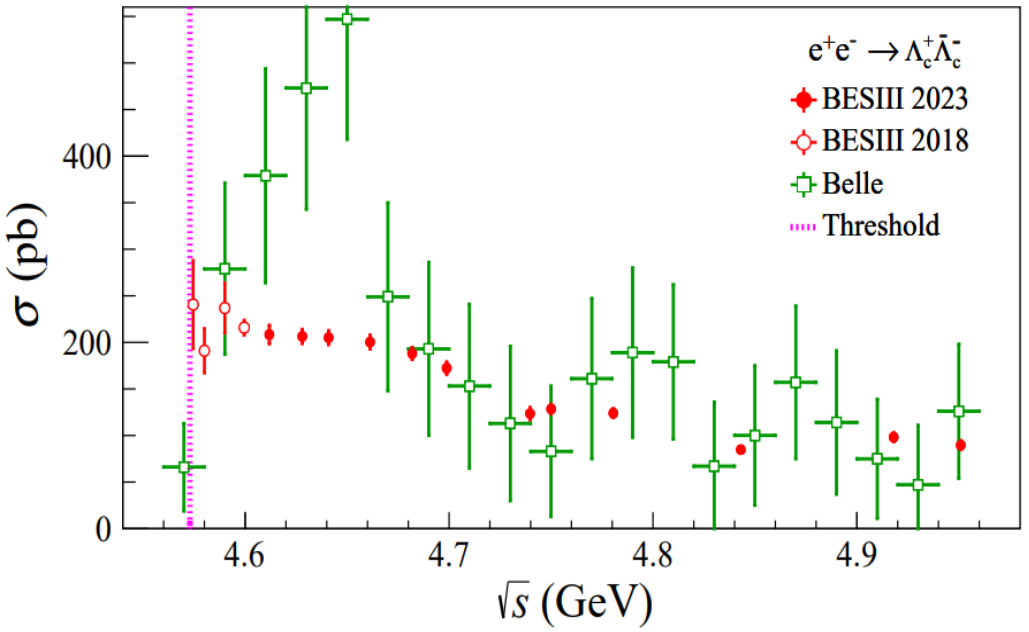

EMFFs of Λ_c^+ and proton

- $|G_E/G_M|$ is consistent with 1 near production threshold
- Similar oscillation in Λ_c^+ $|G_E/G_M|$ distribution as proton observed

$$|G_E/G_M|(s) = \frac{1}{1+\omega^2/r_0}[1 + r_1 e^{-r_2\omega}\sin(r_3\omega)], \quad \omega = \sqrt{s} - 2m_{\Lambda_c}$$

PRL131,191901 (2023)

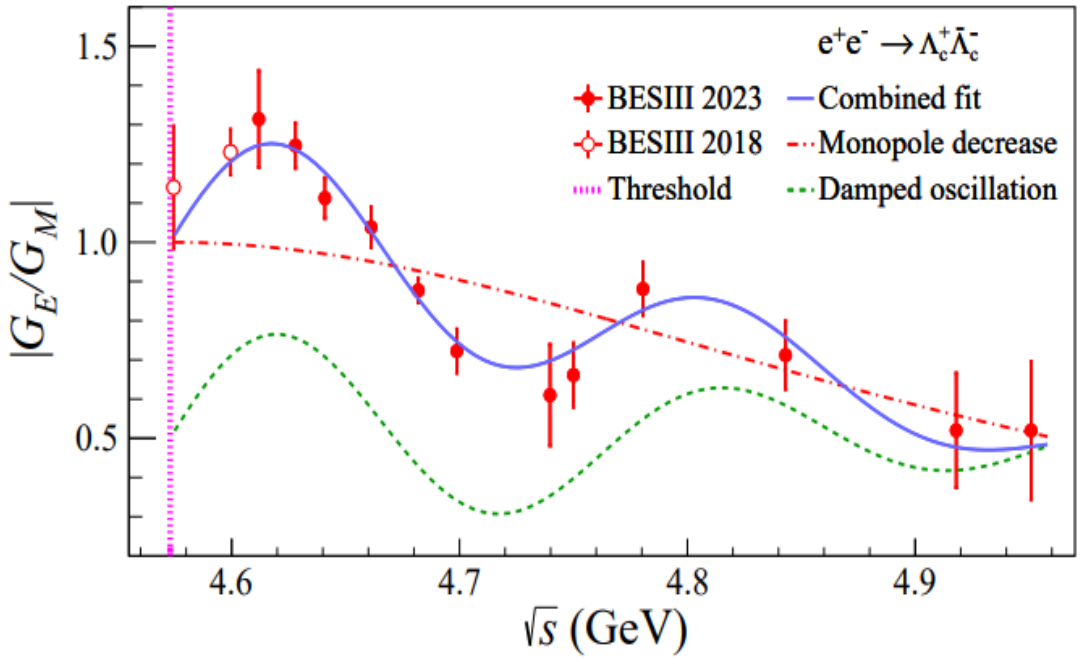

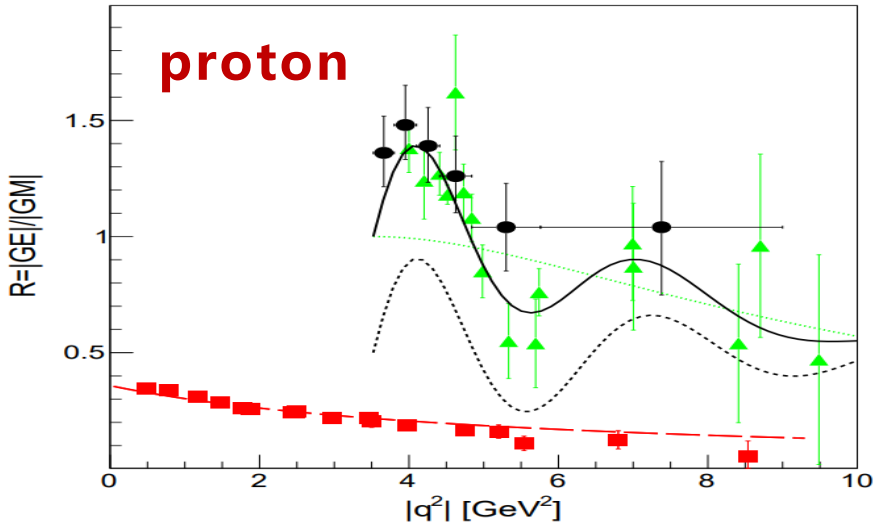

Cross section of $e^+e^- \to \Lambda_c^+ \bar{\Lambda}_c^{*-}$

- $e^+e^- \to \Lambda_c^+ \bar{\Lambda}_c(2595)^- + c.c.$ and $e^+e^- \to \Lambda_c^+ \bar{\Lambda}_c(2625)^- + c.c.$ are measured for the first time at c.m. energies of 4.918 and 4.951 GeV.
- Nonzero cross sections are observed very close to the production threshold.

PRD 109, L071104 (2024)

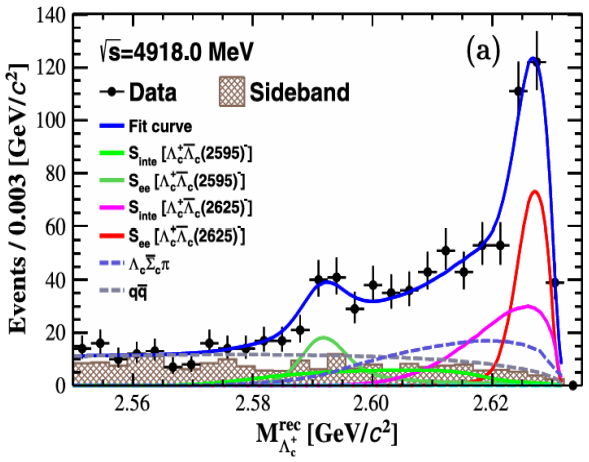

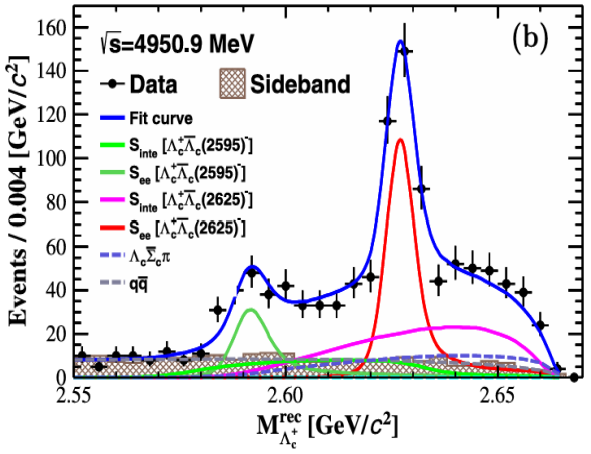

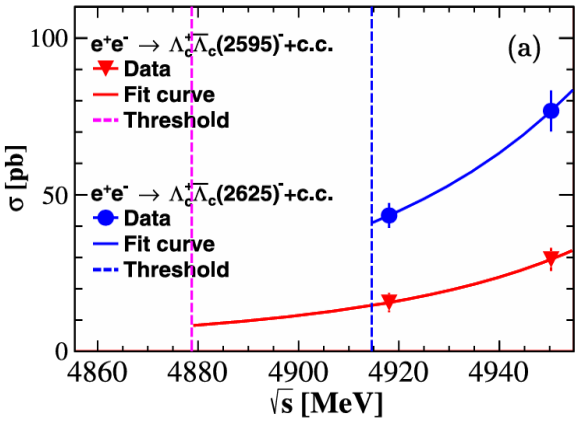

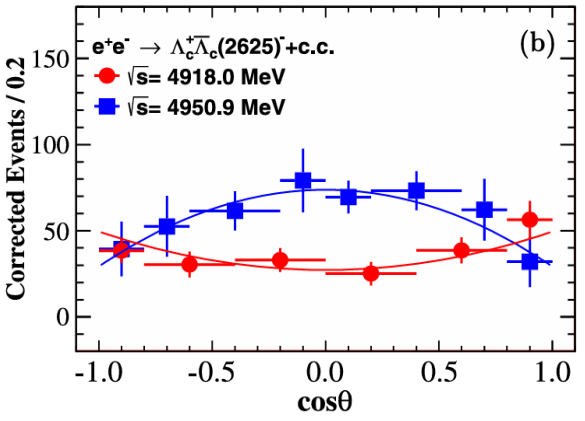

Signal process	$e^+e^- \to \Lambda_c^+\bar{\Lambda}_c(2595)^- + \text{c.c.}$		$e^+e^- \to \Lambda_c^+\bar{\Lambda}_c(2625)^- + \text{c.c.}$	
$\sqrt{s}$ (MeV)	4918.0	4950.9	4918.0	4950.9
N_{sig}	148 ± 29	216 ± 27	311 ± 28	552 ± 47
σ (pb)	$15.6 \pm 3.1 \pm 0.9$	$29.4 \pm 3.7 \pm 2.4$	$43.4 \pm 4.0 \pm 4.1$	$76.8 \pm 6.5 \pm 4.2$
α_{Λ_c}	...	...	$0.82 \pm 0.56 \pm 0.02$	$-0.60 \pm 0.20 \pm 0.01$
$\sqrt{\lvert G_E\rvert^2 + 3\lvert G_M\rvert^2}/\lvert G_C\rvert$	...	...	$5.95 \pm 4.07 \pm 0.15$	$0.94 \pm 0.32 \pm 0.02$

$$\frac{|G_E|^2 + 3|G_M|^2}{|G_C|^2} = \tau \cdot \frac{1 + \alpha_{\Lambda_c}}{1 - \alpha_{\Lambda_c}}.$$

总结和展望

类时重子形状因子研究现状

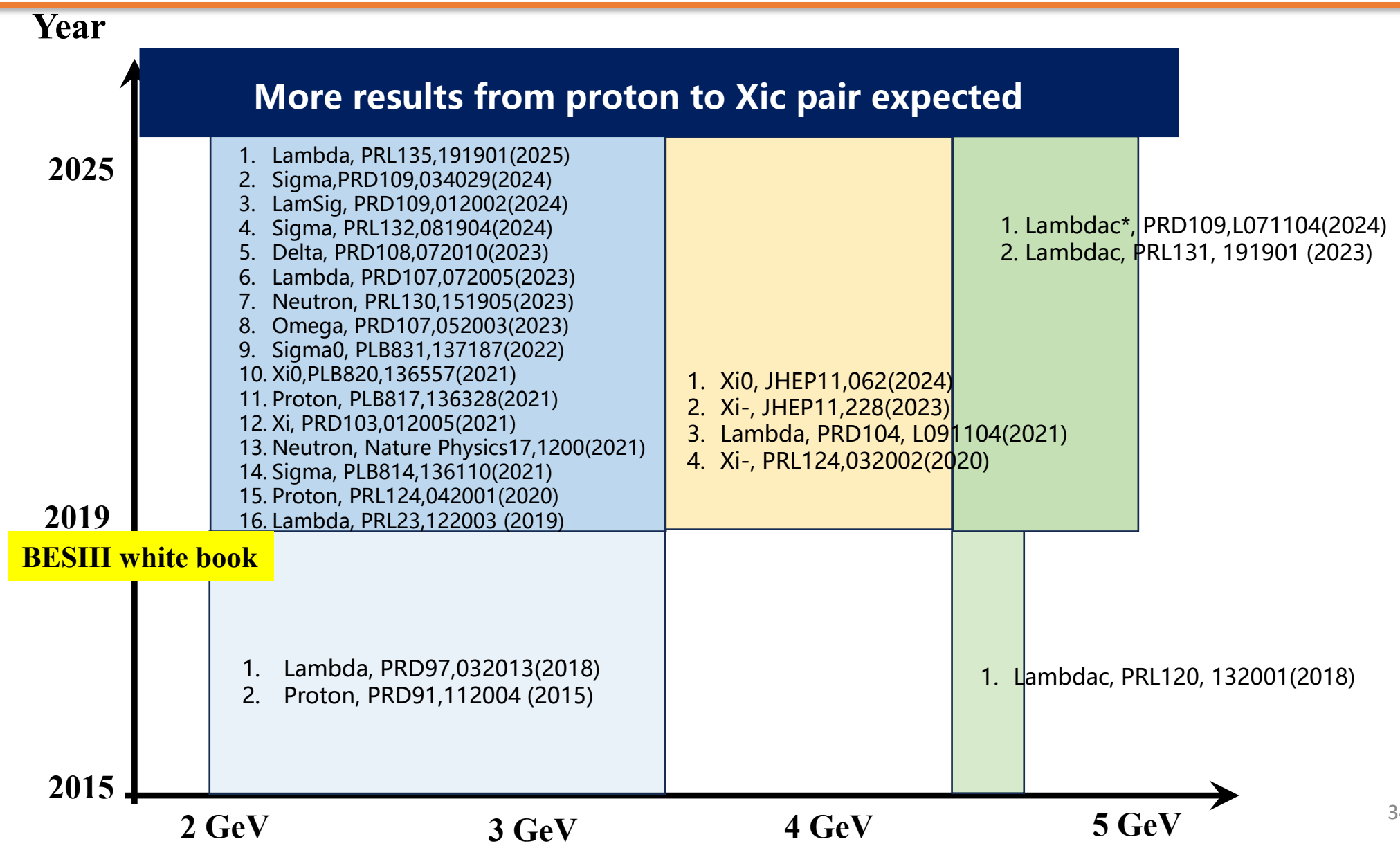

类时重子形状因子研究现状（1）

	Energy scan $e^+e^- \to B\bar{B}$			ISR $e^+e^- \to \gamma_{ISR}B\bar{B}$		
	Effective FF	$\|G_E/G_M\|$ ratio	Relative phase	Effective FF	$\|G_E/G_M\|$ ratio	Relative phase
p	Over 30 energy points, $q \in (1.877, 3.08)$ GeV, best precision: 2% Threshold ongoing	16 energy points, $q \in (2.0, 3.08)$ GeV, best precision: 3% Threshold ongoing	-	c.m.e=3.773- 4.6, 10.58 GeV, $q \in (1.877, 3.08)$ GeV, best precision: 5% New data ongoing	15 energy intervals, $q \in (1.88, 3)$ GeV, best precision: 20% New data ongoing	-
n	~20 energy points, $q \in (1.877, 3.08)$ GeV, best precision: 5%	5 intervals with $q \in (2.0, 3.08)$ GeV, best precision: 20%	-	Ongoing	-	-
Λ	Over 40 energy points, $q \in (2.2324, 4.6)$ GeV, best precision: 2%	6 energy points, $q \in (2.3864, 3.08)$ GeV, best precision: 10%	5 energy points, $q \in (2.3864, 3.08)$ GeV, best precision: 10°	c.m.e=3.773- 4.26, 10.58 GeV, 20 energy intervals, ~500 events New data ongoing	Ongoing	Ongoing
$\Lambda\bar{\Sigma}^0$	14 energy points, $q \in (2.3094, 3.08)$ GeV, best precision: 4%	Ongoing	Ongoing	c.m.e=10.58 GeV, 5 energy intervals, ~25 events New data ongoing	-	-

类时重子形状因子研究现状（2）

	Energy scan $e^+e^- \to B\bar{B}$			ISR $e^+e^- \to \gamma_{ISR}B\bar{B}$		
	Effective FF	$\|G_E/G_M\|$ ratio	Relative phase	Effective FF	$\|G_E/G_M\|$ ratio	Relative phase
Σ^+	8 energy points, $q \in (2.3864, 3.08)$ GeV, best precision: 6%	3 energy points, $q \in (2.36, 3.08)$ GeV, best precision: 20%	3 energy points $q \in (2.3864, 2.90)$ GeV, best precision: 20°	c.m.e=3.773-4.258 GeV, 11 energy intervals, ~180 events New data ongoing	Ongoing	Ongoing
Σ^0	7 energy points, $q \in (2.3864, 3.08)$ GeV, best precision: 6%	Ongoing	Ongoing	c.m.e=10.58 GeV, 5 energy intervals, ~20 events New data ongoing	Ongoing	Ongoing
Σ^-	6 energy points, $q \in (2.396, 3.08)$ GeV, best precision: 12%	-	-	-	-	-
Ξ^0/Ξ^-	~10 energy points, $q \in (2.644, 3.08)$ GeV, best precision: 12%	-	-	Ongoing	-	-
Λ_c^+	16 energy points, , $q \in (4.59, 4.95)$ GeV, best precision: 2%	16 energy points, $q \in (4.59, 4.95)$ GeV, best precision: 4%	13 energy points $q \in (4.6, 4.95)$ GeV, best precision: 4°	/	/	/

实验现象

Updated from Nat.Sci.Rev. 8 (2021) 11, nwab187

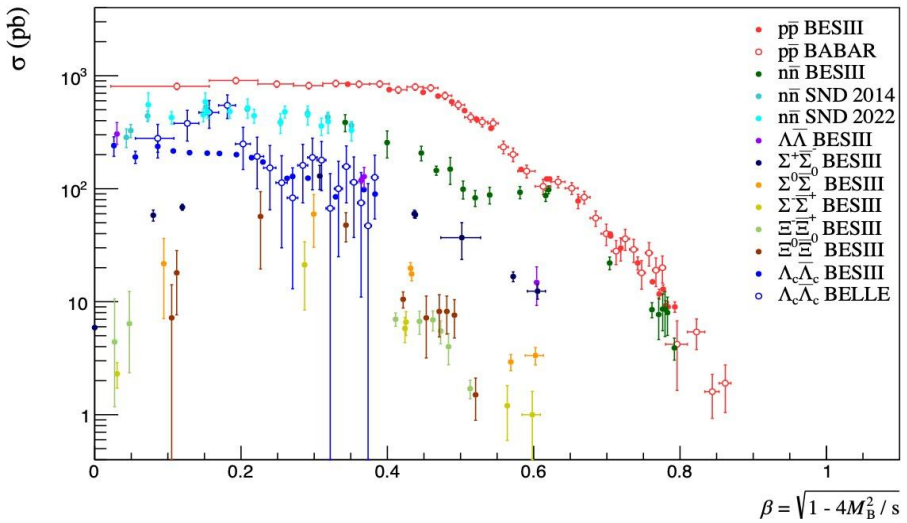

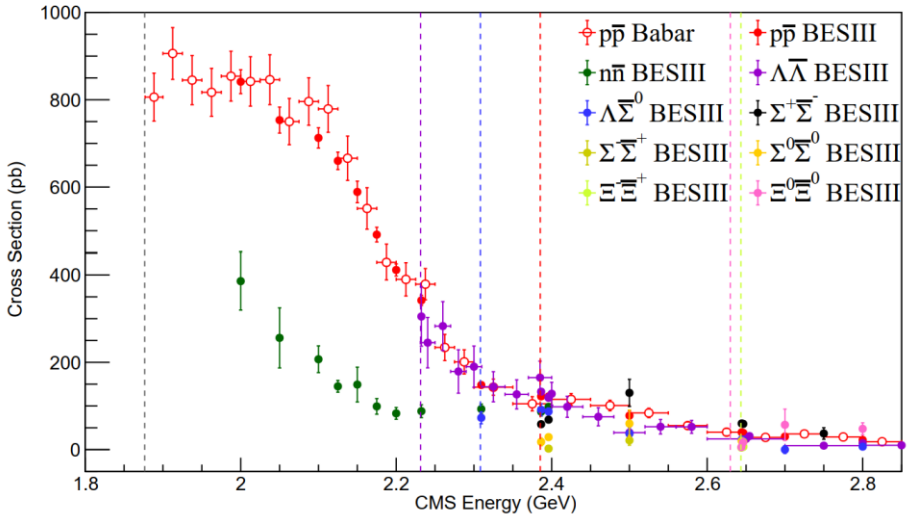

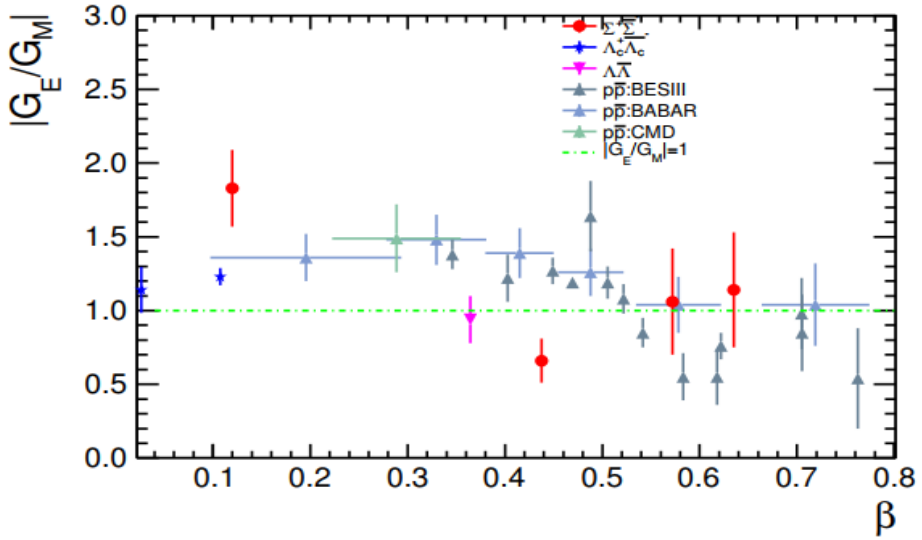

- $p\bar{p}$, $\Lambda\bar{\Lambda}, \Lambda\bar{\Sigma}^0, \Lambda_c^+\bar{\Lambda}_c^-$ 阈值处的反常截面增强
- $p\bar{p}$, $n\bar{n}$ 约化形状因子振荡，和$\Lambda\bar{\Lambda}, \Lambda\bar{\Sigma}^0, \Sigma^+\bar{\Sigma}^-$和$\Xi\bar{\Xi}$ 的耦合
- p, Λ_c^+, Σ^+ 的$|G_E/G_M|$比值阻尼振荡，阈值附近显著大于1
- Λ, Σ^+, Λ_c^+ 的相对相位确定，存在横向极化，然而与理论模型有较大差别

新的机遇

- 确定了超子的电磁形状因子和相位，就能够确定（单光子交换假设下的）超子-反超子系统自旋密度矩阵，检验超子系统中的量子关联 https://indico.itp.ac.cn/event/279/

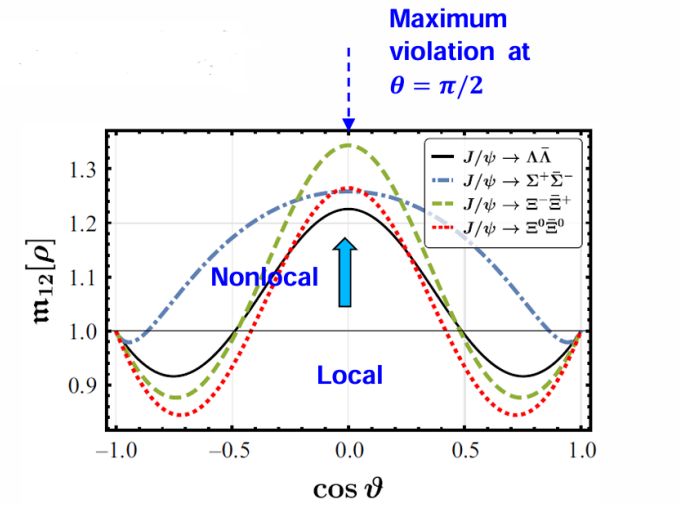

- 利用$e^+e^- \to \gamma B\bar{B}$过程（大部分过程已有现成的信号事例），可以确定GDA（广义分布振幅）和引力形状因子

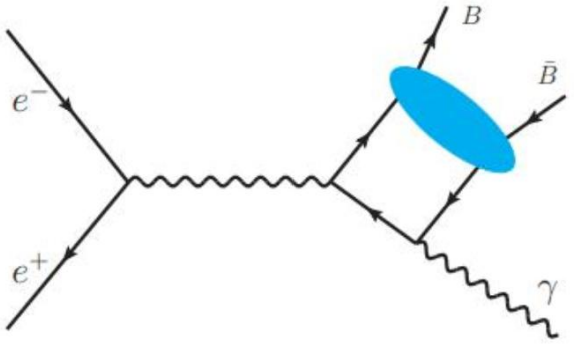

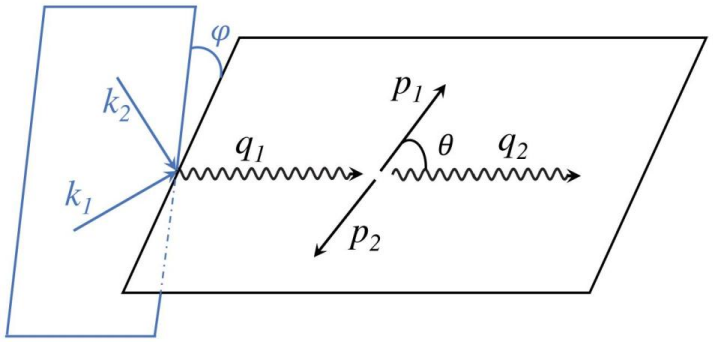

https://indico.itp.ac.cn/event/374/

总结

- BESIII利用能量扫描和初态辐射方法，系统研究了类时空间重子的电磁形状因子，取得了丰富的实验结果
- 实验结果可以检验多种理论模型，如ChPT, VMD, YYbar model；结合形状因子比值和相位，利用色散关系，能够给出模型依赖的重子电磁半径；Y-Ybar系统的自旋密度矩阵也能够完全确定从而构造量子关联各种物理量
- 然而实验观测现象对理论模型提出了挑战，包括阈值效应，约化形状因子的振荡、电磁形状因子比值和相位（极化）随着能量点的演化
- 期待与理论专家的交流，欢迎各位老师提出宝贵意见

Thank you!